

35-32-40W
15-129-21249

PETROGRAPHIC STUDY
FOR
ANADARKO PETROLEUM CORPORATION
CORNELL UNIVERSITY PROJECT
MORTON COUNTY, KANSAS



CORE LABORATORIES



CORE LABORATORIES

PETROGRAPHIC STUDY

FOR

ANADARKO PETROLEUM CORPORATION

**CORNELL UNIVERSITY PROJECT
MORTON COUNTY, KANSAS**

**File: 194274
December 1994**

**Prepared by
Core Laboratories
1875 Monetary Drive
Carrollton, Texas 75006**



PETROLEUM SERVICES

September 21, 1995

Raymond Sorenson / Warren Winters
Anadarko Petroleum Corporation
11th Floor Anadarko Tower
17001 Northchase Drive
Houston, Texas 77060

Subject: Petrographic Study
Project: NMR Cornell University Project
Location: Morton County, Kansas
File Number: 194274

Gentlemen:


This report contains the results of the petrographic study performed on three core samples from a well in Morton County, Kansas, relating to the Cornell University NMR logging project. The study includes general thin section descriptions with photomicrographs prepared in both ordinary transmitted light and fluorescent light, along with X-ray diffraction (XRD) and scanning electron microscopy (SEM) analyses. Elemental compositional data was obtained by energy dispersive spectroscopy during the SEM analysis. The results herein supplement other petrophysical data produced by Core Laboratories for this project. This petrographic study was completed in December of 1994 and a single report was provided at that time.

It has been a pleasure performing this study for Anadarko Petroleum Corporation. We hope that the results will aid in the successful conclusion of your NMR logging project. If you have any questions about this report, or if we can be of further assistance, please feel free to contact us.

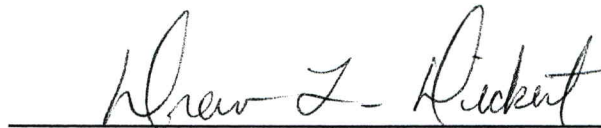
Sincerely,
CORE LABORATORIES
Reservoir Geology/Stratigraphy Group

Drew L. Dickert
Senior Petrologist


PROJECT REVIEW




Mark A. Smesny
Thin Section Preparation



Drew L. Dickert
Petrologist



Malcolm S. Jones
X-ray Diffraction Specialist



Donald G. Harville
Supervisor/Reviewer

TABLE OF CONTENTS

	<u>Page</u>
INTRODUCTION	1
DISCUSSION	1
LITHOLOGY AND PETROGRAPHY	1
POROSITY AND PORE WALL MINERALS	2
ANALYTICAL PROCEDURES	3
THIN SECTION PREPARATION	
SEM/EDS ANALYSIS	3
X-RAY DIFFRACTION ANALYSIS	3
REFERENCES	5

TABLE 1: MINERAL ANALYSIS BY X-RAY DIFFRACTION

THIN SECTION AND SEM PHOTOMICROGRAPHS AND DESCRIPTIONS

- PLATE 1 - Sample 1B; 2530.2 Feet (Thin Section)
- PLATE 2 - Sample 1B; 2530.2 Feet (Thin Section)
- PLATE 3 - Sample 1B; 2530.2 Feet (SEM)
- PLATE 4 - Sample 1B; 2530.2 Feet (SEM)
- PLATE 5 - Sample 2A; 2537.4 Feet (Thin Section)
- PLATE 6 - Sample 2A; 2537.4 Feet (Thin Section)
- PLATE 7 - Sample 2A; 2537.4 Feet (SEM)
- PLATE 8 - Sample 2A; 2537.4 Feet (SEM)
- PLATE 9 - Sample 3B; 2541.7 Feet (Thin Section)
- PLATE 10 - Sample 3B; 2541.7 Feet (Thin Section)
- PLATE 11 - Sample 3B; 2541.7 Feet (SEM)
- PLATE 12 - Sample 3B; 2541.7 Feet (SEM)
- PLATE 13 - Sample 3B1; 2541.7 Feet (SEM)

ENERGY DISPERSIVE SPECTROSCOPY (EDS) PLOTS

- FIGURE 1 - Sample 1B; Mixed layer clay
- FIGURE 2 - Sample 1B; Dolomite
- FIGURE 3 - Sample 2A; Halite
- FIGURE 4 - Sample 2A; Silica
- FIGURE 5 - Sample 3B1; Whole Sample
- FIGURE 6 - Sample 3B1; Illitic clay

INTRODUCTION

Three trimmed ends of whole core plugs from an unspecified well in Morton County, Kansas, were received by the Reservoir Geology Group of Core Laboratories in Carrollton, Texas, for petrographic analyses. The samples are from the depths of 2530.2, 2537.4, and 2541.7 feet. Thin section petrography with fluorescence microscopy, scanning electron microscopy (SEM) with energy dispersive spectrometry (EDS), and X-ray diffraction (XRD) analyses were performed on these samples. The analyses serve to evaluate the textural, mineralogic, and porosity characteristics of the cored intervals represented by these samples. Plates 1 through 13 contain the thin section and SEM photomicrographs along with their accompanying descriptions. Figures 1 through 6 display the EDS spectra (elemental compositions) for the various minerals in contact with the pore fluids. Table 1 shows the results of the X-ray diffraction analysis for bulk sample mineral composition. The following discussion summarizes the data.

DISCUSSION

Lithology and Petrography

The three samples are all silty to sandy, partially neomorphosed limestones. According to the classification of Dunham (1962), the depositional texture of the samples is grainstone, or perhaps packstone for Samples 1B and 3B. Original carbonate mud matrix (micrite) that may have been present in each sample has been neomorphosed to calcite microspar. Moderate amounts of matrix may have been present in Sample 1B and lower amounts in Sample 3B. Sample 2A seems to have contained very little original carbonate mud matrix. By the classification of Folk (1980) these limestones can be considered biomicroparites.

Allochem grains are abundant and include common skeletal fragments, algal oncolites, and peloids. The skeletal fragments consist of important contributions of echinoderms, mollusks, foraminifers, bryozoans, and brachiopods. Many of the skeletal allochems, especially the foraminifers, have been heavily micritized. Peloids are micritic grains of uncertain origin, although many may be micritized, unrecognizable skeletal fragments. Algal oncolites are larger allochems (up to a few millimeters in these samples) that have nuclei of skeletal grains and/or peloids wrapped with layers of algal-bound micrite. The allochems in these limestones range in size from about 0.06 to 4.32 millimeters, with averages ranging between approximately 0.32 and 0.50 millimeters.

The detrital siliciclastic grains range from medium silt through very fine sand size. Sample 2A contains much more sand than the other two samples. X-ray diffraction analysis (Table 1) indicates a total of 42 percent siliciclastic minerals for Sample 2A, in the form of quartz, plagioclase and potassium feldspar. Siliciclastics make up only 7.7 to 9.4 percent of the other two samples. A small portion of these totals is in the form of authigenic quartz and feldspar.

The allochems and siliciclastic grains are cemented by abundant calcite microspar, some of which may be neomorphosed micrite matrix. Finely to coarsely crystalline

calcite and lesser dolomite also occur as cements, filling larger pores. Authigenic minerals that occur in minor to rare amounts are quartz, pyrite, hematite, gypsum/anhydrite, illitic clay, halite, feldspar, and titanium oxide. Quartz and feldspar occur primarily as overgrowths on detrital grains. Pyrite and hematite occur as tiny crystals scattered throughout the pore system. The hematite tends to be concentrated around and within the oncolite grains. Gypsum/anhydrite are present as widely separated, pore-filling patches of coarser crystals. Flaky to fibrous, illitic clay minerals partially coat some microspar and micrite crystals (e.g., Plates 3B and 4). Although very minor, the clay seems most common in Sample 1B, according to SEM and XRD analyses.

Porosity and Pore Wall Minerals

The pores types in the three limestones analyzed in the petrographic study include intercrystal, micro-intercrystal, interparticle, intraparticle, moldic, and intergranular pores. Interparticle pores and intercrystal pores are often commingled because of the presence of common microspar and spar cements in the interparticle spaces. Micro-intercrystal pores are common in the micritized allochems and algal oncolites. Intraparticle pores are typically seen in foraminifer tests that have not been filled with cement. Moldic pores represent dissolved allochems of probable skeletal origin. Sample 2A appears to have the highest porosity, due to the addition of common intergranular pores created by the abundant sand component. This sample should also have the highest permeability because of larger and better interconnected pores. Sample 1B has the lowest porosity, due to stylolitization and associated greater cementation.

Table 1 quantifies the important minerals in each of the limestones. Additional minerals not detected by XRD analysis, but seen in the thin section or SEM analysis of each sample, include hematite, anhydrite, and titanium oxide. Gypsum and halite were detected in small amounts in all three samples by either XRD, SEM or thin section analysis. Halite was not detected in thin section, but was detected by SEM and/or XRD analyses. The lack of detection of halite and gypsum by all the analyses probably is indicative of the scattered occurrences of these minerals. Sample 3B, which contained the most halite by SEM analysis, was analyzed a second time by SEM analysis of an inner-core end trim from a sample plug drilled in oil (Sample 3B1; Plate 13). No halite was detected over an approximate surface area of one centimeter square.

All of the minerals identified in this study should be present along pore walls and, thus, have some contact with the pore fluids. Pore wall surface area is dominated by tiny crystals of calcite (e.g., Plates 3B and 13B). Sample 2A has significant pore surface area composed of quartz and feldspar, in addition to calcite. Minerals least interactive with the pore system are probably gypsum and anhydrite, due to their coarser size and sparsely spaced occurrence. Dolomite (sometimes iron rich), pyrite, hematite, illitic clay, and halite are all in contact with pore fluids, but these minerals occur in minor to trace amounts. The EDS spectra at the end of the report (Figures 1 through 6) show qualitative elemental compositions of some of the pore wall minerals in these limestones.

ANALYTICAL PROCEDURES

A petrographic study allows for the characterization of reservoir rock textures, mineralogy, and porosity. Information about the relationships among rock textures, framework grains, matrix, cement, and porosity are determined from thin section analyses. X-ray diffraction analysis provides the identities and quantities of specific rock-forming minerals. Scanning electron microscopy (SEM) provides very high-magnification views with excellent depth of field of framework grains, cements, matrix, authigenic clays, and pores, from which mineral morphologies (particularly clays) and porosity types and distribution are identified and described. Energy dispersive spectroscopy (EDS) provides the qualitative elemental analyses of mineral phases and allows for positive identification of cements, matrix, and authigenic clays observed during the SEM observation.

Thin Section Preparation

The dried sample fractions were prepared for thin section analysis by first impregnating them with an epoxy resin containing a magenta-stained, fluorescent dye (Rhodamine B) to highlight the pore space. After curing, each of the samples was mounted on a frosted glass slide and then cut and ground in water to an approximate thickness of 30 microns. The thin sections were analyzed using standard petrographic techniques. The petrographic terminology used in this report is that of Dunham (1962) and Folk (1980). Photomicrographs were obtained by use of a Leitz Orthoplan petrographic microscope, equipped for fluorescence microscopy. A second set of thin sections was prepared using blue-dyed (Columbia Blue). This set, which was not photographed, was prepared from inner-core end trims of plugs drilled in oil, for purpose of preserving any halite. These thin sections were subsequently ground in oil.

SEM/EDS Analysis

For the SEM/EDS study, the samples are broken to form fresh surfaces. Each sample is then mounted on an aluminum stub and coated with a thin film of gold-palladium (Au-Pd) alloy using a Polaron sputter coater. The SEM photomicrographs are secondary electron images taken with a Polaroid camera attached to an ISI-SX-40 Scanning Electron Microscope operating at 20kV. Qualitative elemental data of selected phases observed during the SEM study are obtained through the use of an interfaced Tracor Northern TN 5400 Energy Dispersive Spectroscopy Unit equipped with an Si (Li) detector. Recognition of authigenic clays is based on the criteria proposed by Wilson and Pittman (1977).

X-ray Diffraction Analysis

A sample selected for bulk X-ray diffraction analysis is dried and cleaned of obvious contaminants. For the present study, the solvent used was toluene, because the oil-drilled samples needed to be cleaned in a fluid that would not dissolve halite. The sample is dried and then milled to pass a 40 mesh sieve. The powdered sample is run on a Philips APD 3600 diffractometer. The resultant diffractograms are analyzed for mineral content using a profile-fitting algorithm. The integrated areas from the profile-fitting algorithm are entered into a spreadsheet which contains correction coefficients for

numerous minerals. These coefficients were obtained according to the adiabatic method outlined by Chung (1974). Tabular data are reported in weight percent format in Table 1.

REFERENCES

Chung, F.H. (1974) A new X-ray diffraction method for quantitative multicomponent analysis. *Advances in X-ray Analysis*. 17, p. 106-115.

Chung, F.H. (1974) Quantitative interpretation of X-ray diffraction patterns of mixtures. I. Matrix-flushing method for quantitative multicomponent analysis. *Journal of Applied Crystallography*, 7, p. 519-525.

Chung, F.H. (1974) Quantitative interpretation of X-ray diffraction patterns of mixtures. II. Adiabatic principle of X-ray diffraction analysis of mixtures. *Journal of Applied Crystallography*, 7, p. 526-531.

Dunham, R.J. (1962) Classification of carbonate rocks according to depositional texture, in W.E. Ham, ed., *Classification of carbonate rocks*. AAPG Memoir 1, p.108-121.

Folk, R.L. (1980) *Petrology of Sedimentary Rocks*. Hemphill Publishing Company, Austin, Texas, 184p.

Wilson, M.D. and Pittman, E.D. (1977) Authigenic clays in sandstones: recognition and influence of reservoir properties and paleoenvironmental analysis: *Journal of Sedimentary Petrology*, vol. 47, p. 3-31.

Anadarko Petroleum Corporation
Cornell University Project

Table 1
Mineral Analysis by X-ray Diffraction

File: 194274

Sample Number	Depth, feet	Quartz	K feldspar	Plagioclase	Calcite	Dolomite	Siderite	Pyrite	Anhydrite	Halite	Gypsum	Total Clay
1B	2530.2	7.7	0.0	0.0	85.3	3.1	0.0	0.4	0.0	0.3	2.0	1.2
2A	2537.4	29.5	5.1	7.4	55.6	1.7	0.0	0.2	0.0	0.5	0.0	0.0
3B	2541.7	8.1	0.0	1.3	87.5	0.1	0.0	1.0	0.0	0.0	2.0	0.0

Note: The data in this table is reported to the nearest tenth of a % to indicate halite values.
The detection limit for halite is about 0.1%; whereas most other minerals are at 1%.

THIN SECTION AND SCANNING ELECTRON MICROSCOPY PHOTOMICROGRAPHS AND DESCRIPTIONS

The scale of the thin section photomicrographs in each plate is a function of the magnification:

79X: Horizontal width of the photomicrograph (127mm) represents 1.607mm.

200X: Horizontal width of the photomicrograph (127mm) represents 0.635mm.

Symbols appear at the bottom of all SEM photomicrographs in this report. From left to right, these symbols are the following: SEM electron accelerating potential in kilovolts (20kV), magnification (X1000), bar scale (microns), and photograph exposure number.

PLATE 1

Thin Section Photomicrographs

Sample 1B

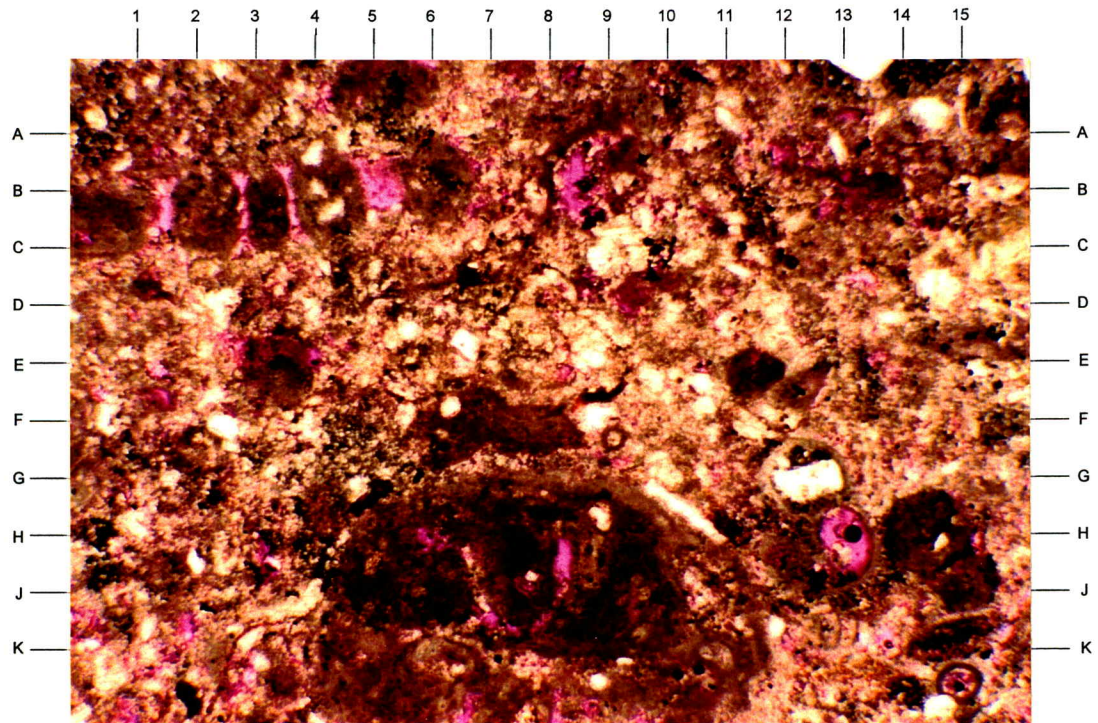
Depth: 2530.2 Feet

A

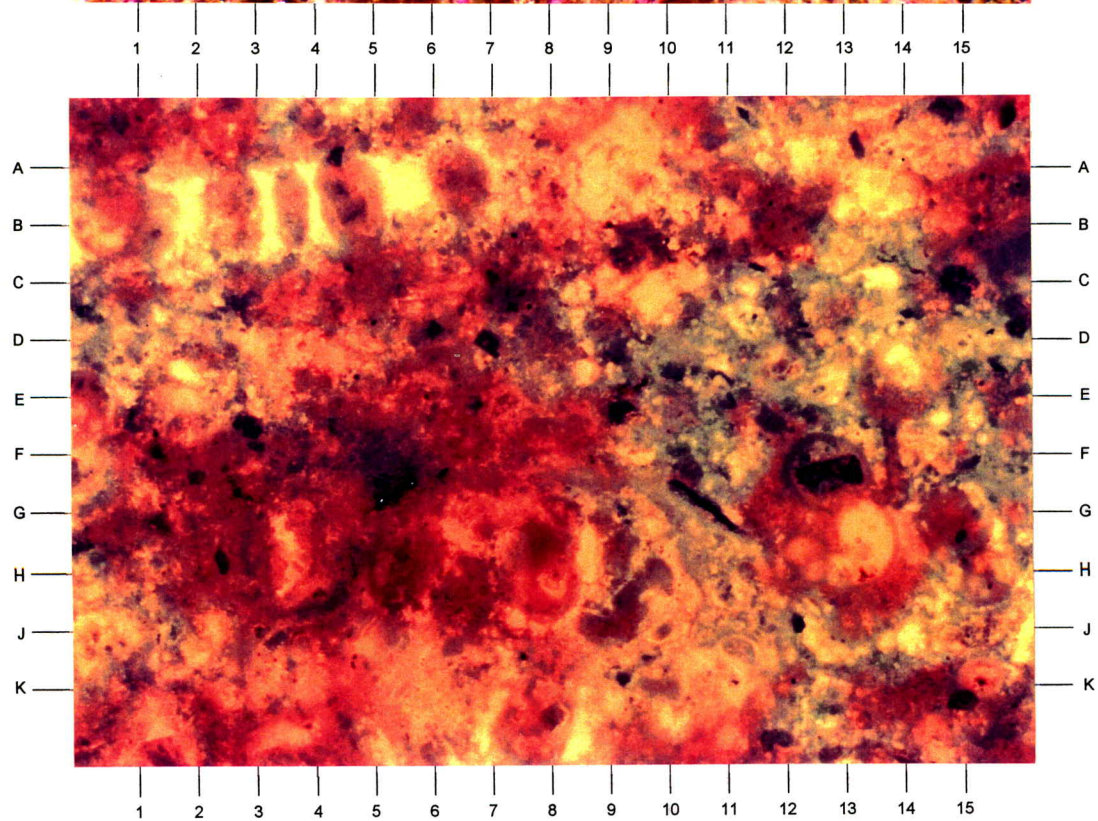
Rock Type:	Silty/sandy limestone
Rock Name: (Dunham, 1962) (Folk, 1980)	Silty/sandy, peloid oncolite skeletal grainstone/packstone Silty/sandy, peloid oncolite biomicrosparite
Average Allochem Size: (estimated)	0.32-0.45 mm (medium sand-size); range = 0.06-2.05 mm
Allochem Sorting:	Poor
Allochem Types:	Common algal oncolites (bottom-G4-11), peloids (B-C1-4?, E-F3.5, E11.5, H15), echinoderms, mollusks, foraminifers (G-J12-13), bryozoans, and brachiopods; possibly minor intraclasts
Terrigenous Grains:	Fairly common silt to very fine sand (mainly quartz; minor potassium feldspar and plagioclase; traces of heavy minerals and mica; rare rock fragments); traces of organic material (G-H5, E-F9)
Matrix:	Original carbonate matrix, if any, has been neomorphosed to microspar
Authigenic Minerals:	Abundant calcite microspar; minor finely to coarsely crystalline calcite and dolomite; minor to trace amounts of pyrite, hematite, quartz (including overgrowths), gypsum (XRD), clay minerals (SEM), and anhydrite; rare titanium oxide and halite (XRD)
Porosity Types:	Abundant intercrystal/interparticle and micro-intercrystal pores (e.g., bottom-J1-3); minor to common intraparticle (A-B8.5, H13) and moldic pores (B-C1-5); traces of intergranular pores and possibly natural microfractures (pore space is colored magenta)
Structures:	Common stylolites (not shown) along which hematite, organics, pyrite, and possibly clays are concentrated
Comments:	Very fine hematite is often concentrated around or within oncolites; many skeletal grains are micritized
Magnification:	79X, transmitted light

B

Under fluorescent light, the epoxy-impregnated pore network shows up with a bright gold color. Many of the larger pores (A-B5.5, G-H13.5, G-H8.5, A-B9) are interconnected by networks of small intercrystal or micro-intercrystal pores (H-K9-13) that are not readily visible with regular transmitted light. Even some areas that are highly micritic contain considerable microporosity (compare the area bottom-J5-7 in photos A and B). (79X, fluorescent light)



A



B

PLATE 2

Thin Section Photomicrographs

Sample 1B

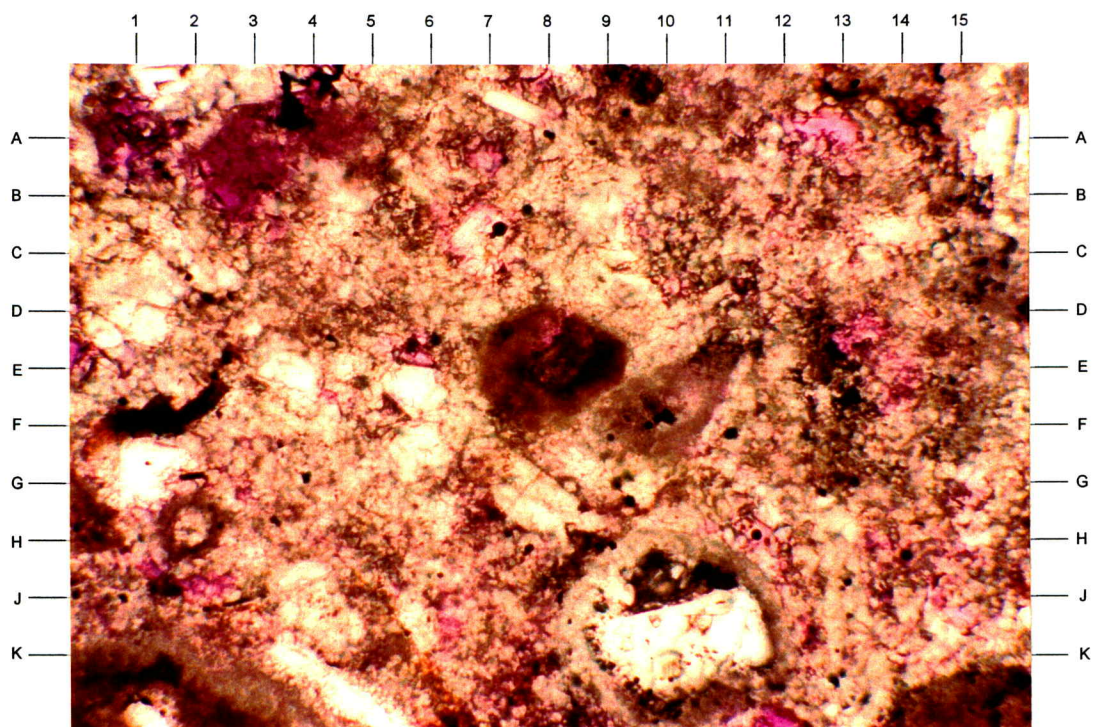
Depth: 2530.2 Feet

A

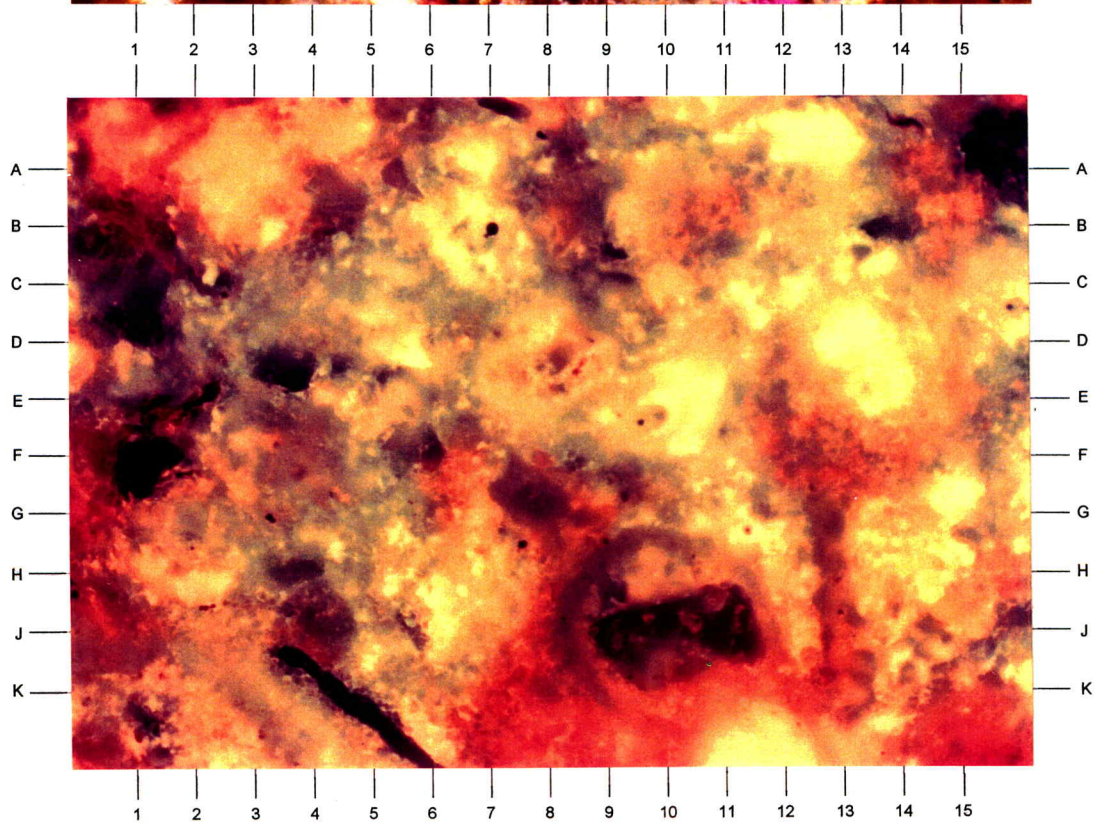
This enlargement of the area surrounding E-F11-12 in Plate 1A reveals the abundance of micro-intercrystal pores that are contained in areas that do not appear very porous in a lower magnification image. Hints of magenta color within the microspar matrix (e.g., H-K6-8) indicates the micropore system has been impregnated with fluorescent-dyed epoxy. Medium crystalline calcite or dolomite has filled a portion of a foraminifer test (J-K9-12). Detrital silt grains appear at G1, E3-4, and top-A7-8, along with minor organic debris (F1, top-A13-14). (200X, transmitted light)

B

The fluorescent light view of Plate 2A shows the extensive, interconnected nature of the micro-intercrystal pore system. Pore space appears bright gold. Pores are so abundant in some micritic allochems that the whole area occupied by the allochem appears bright gold (E-F9-11). Although considerable porosity is evident, permeability should be relatively low due to the very small sizes of most of the pores. Also, irreducible water saturation is likely to be high for this type of pore system. (200X, fluorescent light)



A



B

PLATE 3

SEM Photomicrographs

Sample 1B

Depth: 2530.2 Feet

A

The majority of the mineral components of this limestone sample consists of calcite microspar (A-H2-3, A6 to H8, A-C11-14, H-K10-12) that surrounds allochems that have been altered to micrite or microspar (D-G3-6, A-E7-10, C-F12-15). Larger intercrystal/interparticle pores are common (A6, B14, C-D11, G15), some of which have elongate trends around allochems (C3 to G-H1, B6 to H8). Interconnections among these larger pores are generally restricted to micro-intercrystal pores within the microspar and micrite (see Photo B). Notice the rhombic ferroan dolomite crystal partially filling a pore at F-G13-14. (350X)

B

This is a high-magnification image of the area near B-C10 in Plate 3A. The calcite crystals revealed here are all about four or five microns in size. Numerous micro-intercrystal pores occur among the crystals. Flakes and fibers of apparently authigenic, illitic clay (G3, G5.5, E10.5) are present in trace amounts in many of these microcrystalline areas. The clay contains potassium, with lesser magnesium and iron, in addition to abundant silicon and aluminum. (5000X)

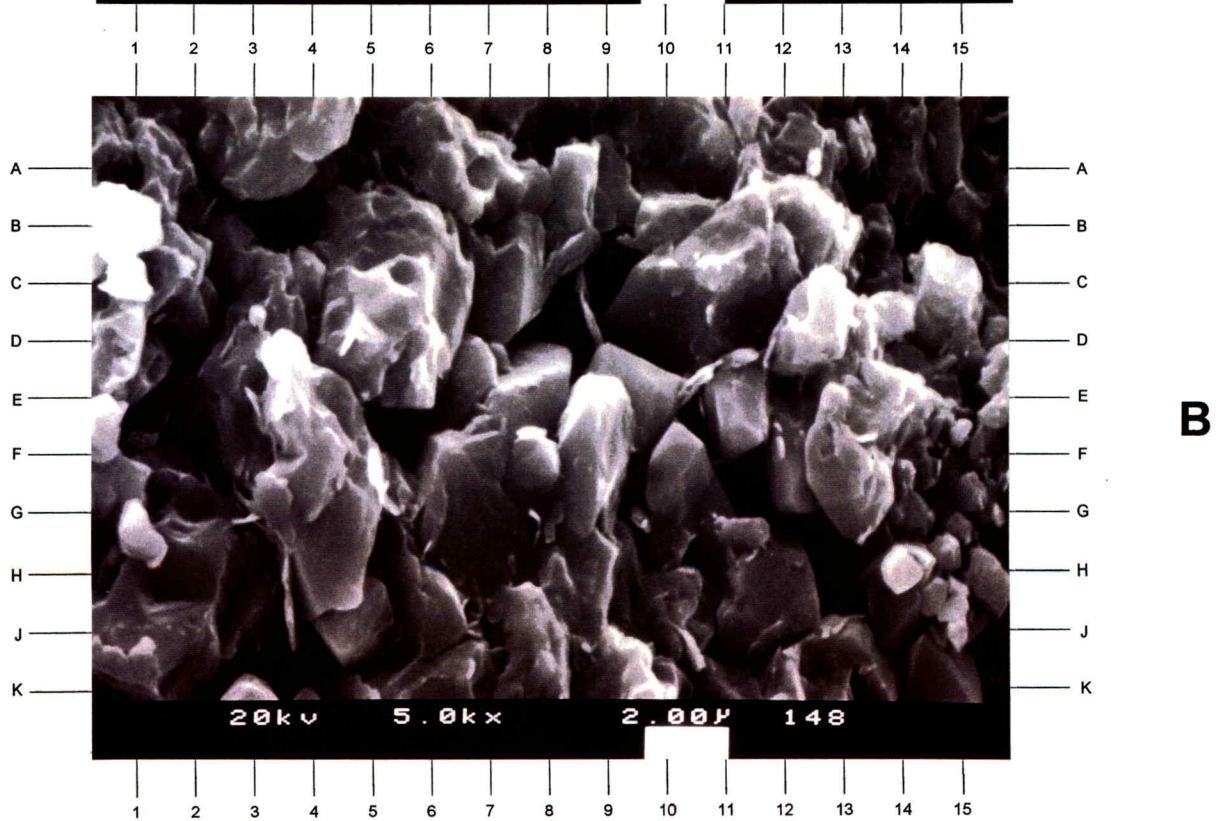
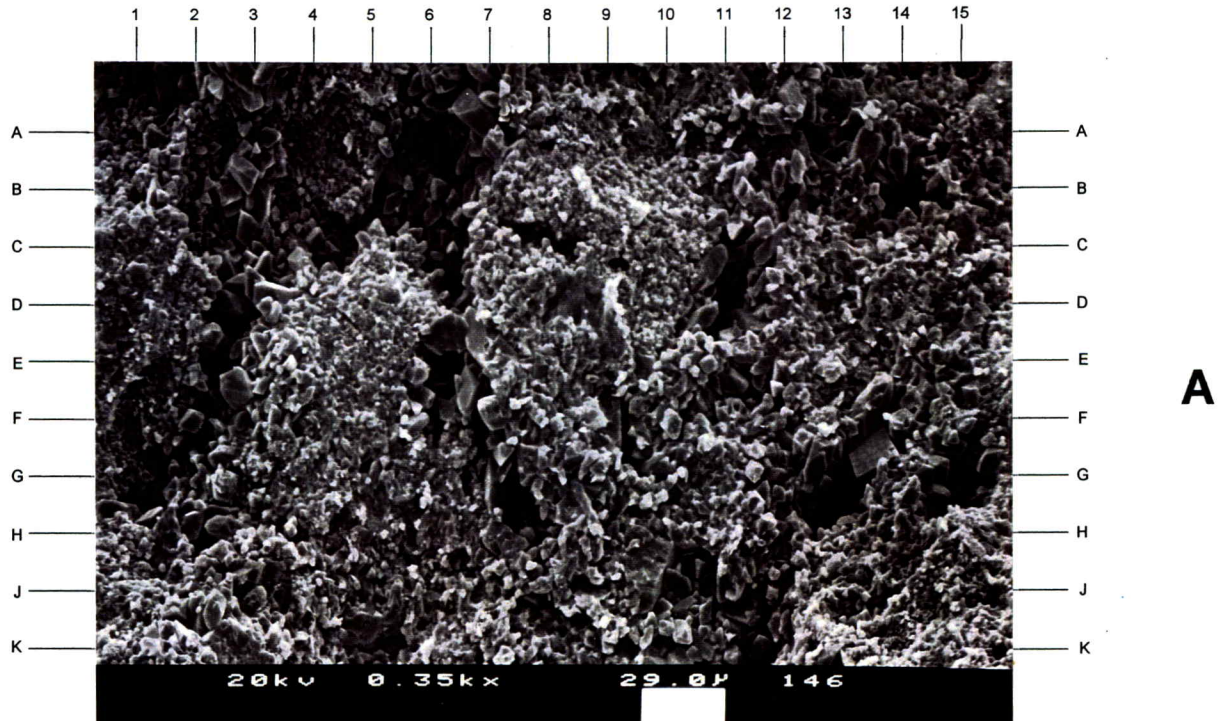


PLATE 4

SEM Photomicrographs
Sample 1B
Depth: 2530.2 Feet

A

The more micritic areas of the sample seem to have the most authigenic clay. The abundant calcite crystals, most less than three of four microns in size, are coated with interlocking flaky to fibrous clay in many portions of this view (C-D5-6, E-J7-8, J-K10). According to EDS analysis, this clay contains silicon, aluminum, iron, potassium, and magnesium. Its chemistry and morphology indicate that it is probably a type of mixed-layer illite/smectite. A rhombic dolomite crystal is present at A3. (4000X)

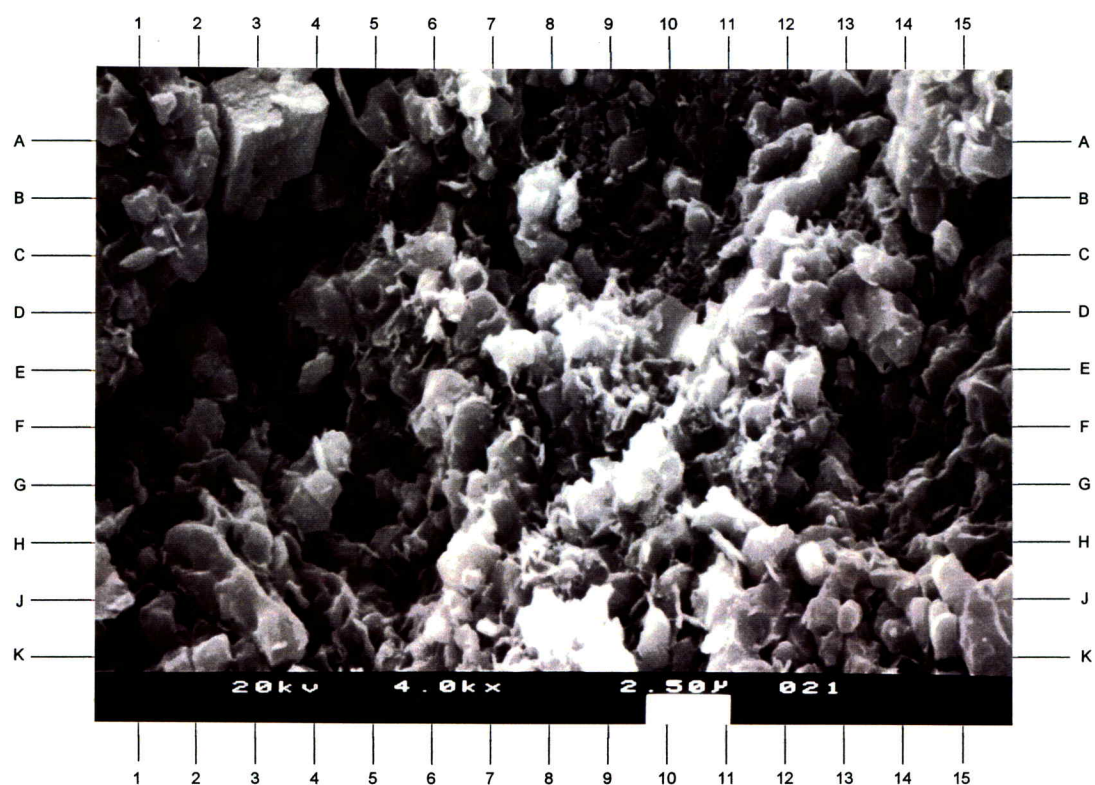


PLATE 5

Thin Section Photomicrographs

Sample 2A

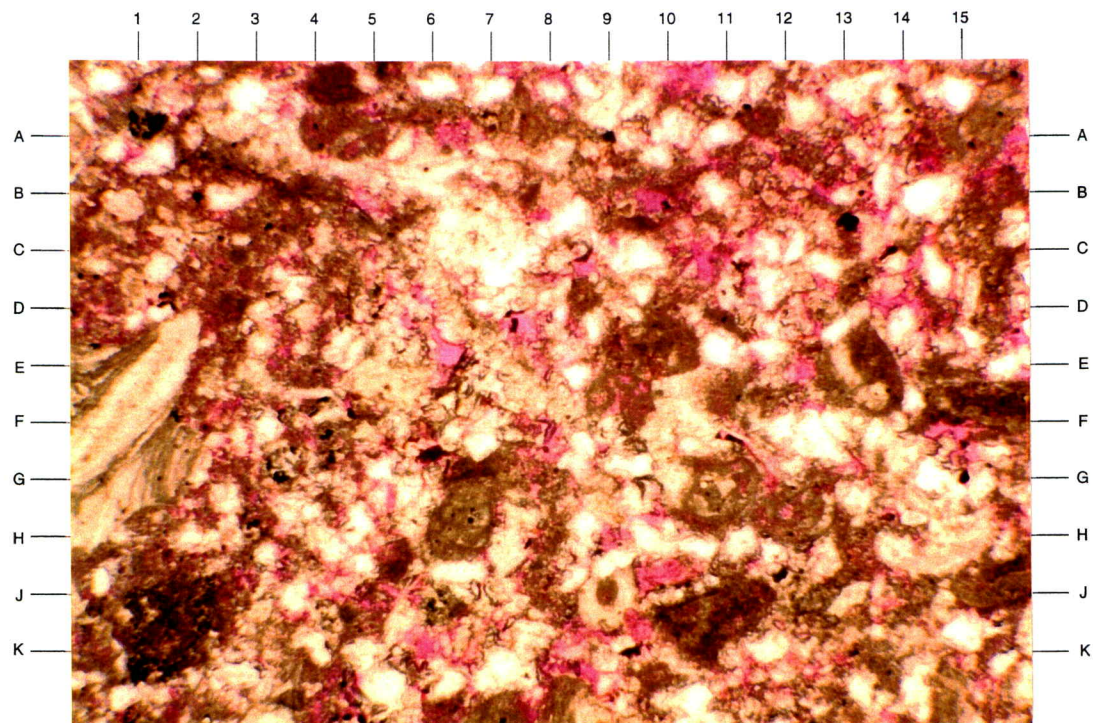
Depth: 2537.4 Feet

A

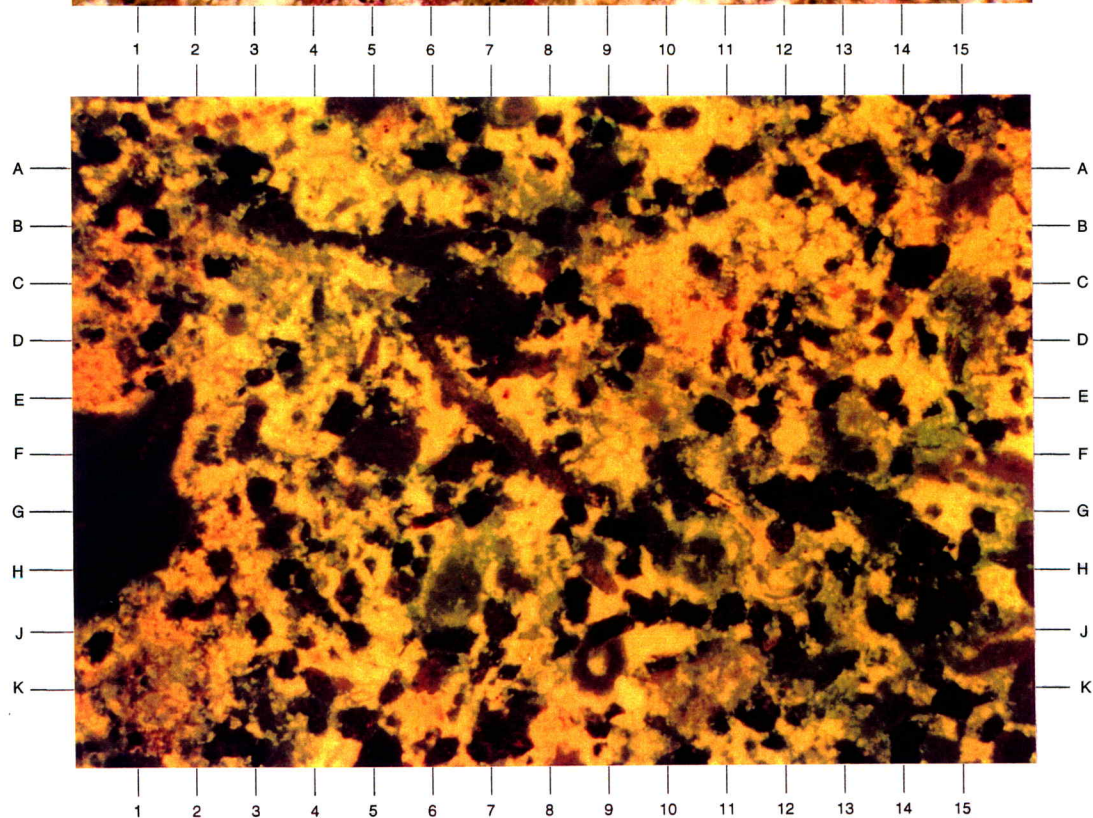
Rock Type:	Sandy limestone
Rock Name:	
(Dunham, 1962)	Sandy, peloid oncolite skeletal grainstone
(Folk, 1980)	Sandy, peloid oncolite biomicrosparite
Average Allochem	
Size: (estimated)	0.32-0.50 mm (medium sand-size); range = 0.06-4.32 mm
Allochem Sorting:	Poor
Allochem Types:	Common algal oncolites, peloids (J-K10.5, D-E10), echinoderms, mollusks, foraminifers (G-H11, G-H12, H6.5), brachiopods (E-H1), and bryozoans; traces of possible intraclasts
Terrigenous	
Grains:	Abundant, well sorted, very fine sand to coarse silt (abundant quartz; common potassium feldspar and plagioclase; traces of heavy minerals and mica; rare rock fragments); traces of organic material
Matrix:	Original carbonate matrix, if any, has been neomorphosed to microspar
Authigenic	
Minerals:	Common calcite microspar (J12, B9); less common finely to coarsely crystalline calcite and dolomite; minor to trace amounts of quartz (especially overgrowths), hematite, anhydrite, gypsum, pyrite, clay minerals (SEM), feldspar overgrowths, and halite (SEM, XRD); rare titanium oxide
Porosity Types:	Common to abundant intercrystal/interparticle to micro-intercrystal pores and intergranular pores (most magenta-colored areas); common intraparticle pores (E-F9-10); minor skeletal-moldic pores
Structures:	None apparent
Comments:	Very fine hematite is often concentrated around or within oncolites; many skeletal grains are micritized; minor concentrations of organic material are present
Magnification:	79X, transmitted light

B

The fluorescent light highlights the abundant pores (bright gold color). This sample has a fairly well interconnected system of small, interparticle/intercrystal and intergranular pores, although pore throats (D-E6, F-G4) are commonly very thin. This sample appears to have higher reservoir quality than the other two samples examined petrographically. Sand and silt grains appear very dark in this photomicrograph. (79X, fluorescent light)



A



B

PLATE 6

Thin Section Photomicrographs

Sample 2A

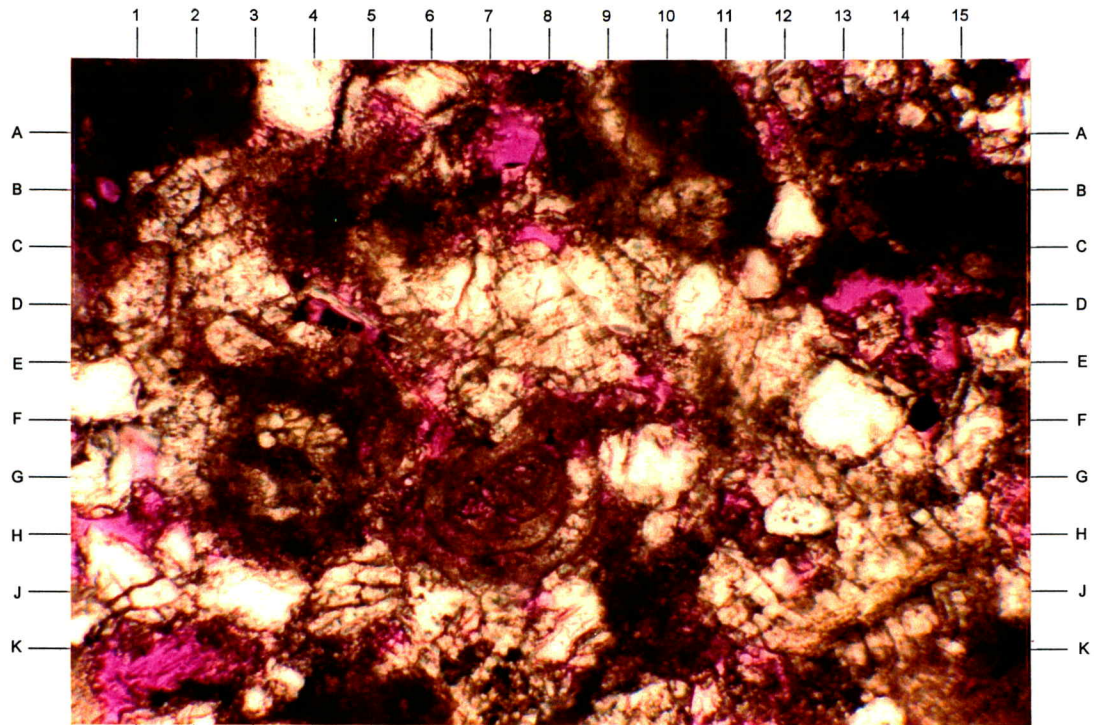
Depth: 2537.4 Feet

A

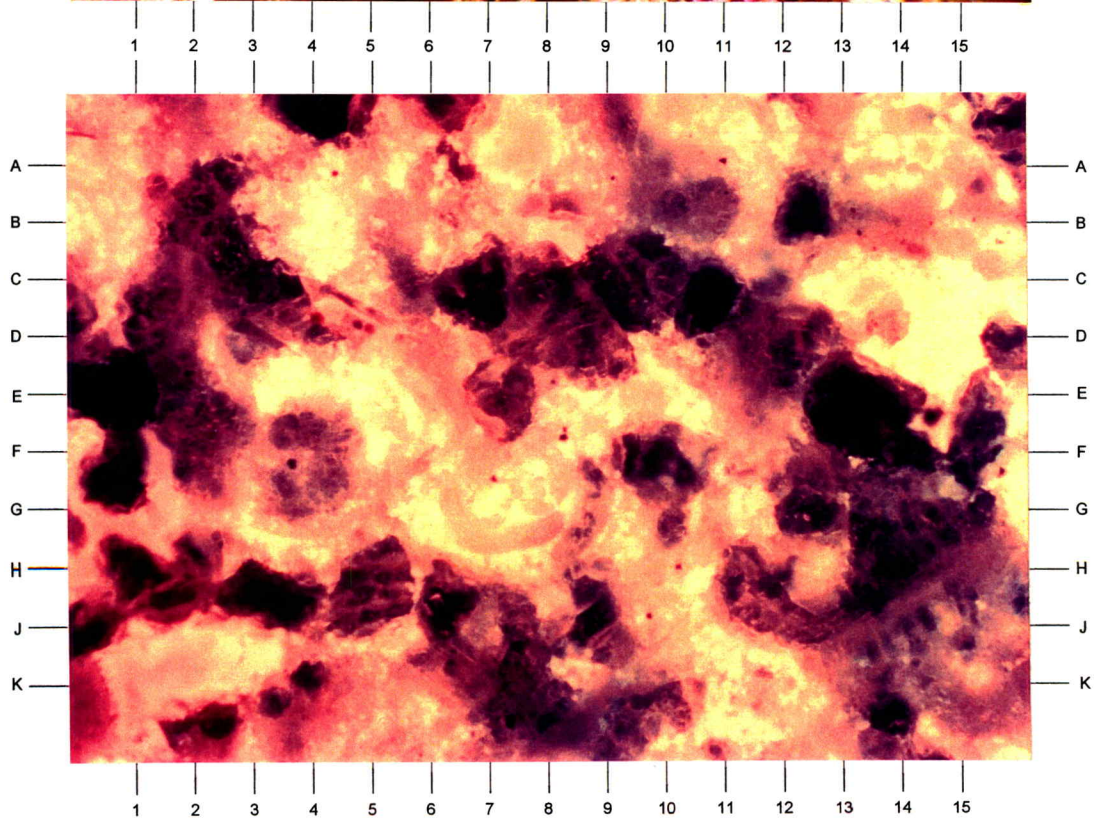
A higher magnification image of the portion of Plate 5A near G13 is provided in this photomicrograph. The allochems visible here are peloids (A1, A10.5, B-C15) and probable micritized and recrystallized foraminifers (F-H3-5, F-H6-8). Sand and silt are common (white grains; E-F0.5, F13). Much of the calcite in the view is microspar or micrite, but some is finely to medium crystalline calcite (C-D2-3, D-E8). The magenta-stained pore system is fairly well developed. (200X, transmitted light)

B

The fluorescent light image of Plate 6A shows the pore system as bright gold in color. Larger open pores (top-A7-8, C-D13-15) are linked by thin pore throats (B9 to B-C12, J4, H-J5.5-6) or by networks of micro-intercrystal pores (F11-12). Notice that many micritized allochems that appear dark in Plate 6A actually contain abundant micro-intercrystal pores and, thus, fluoresce brightly in this view (top-A10-12, D-E3-6). Microporous micritic allochems are likely to contain appreciable bound water. (200X, fluorescent light)



A



B

PLATE 7

SEM Photomicrographs

Sample 2A

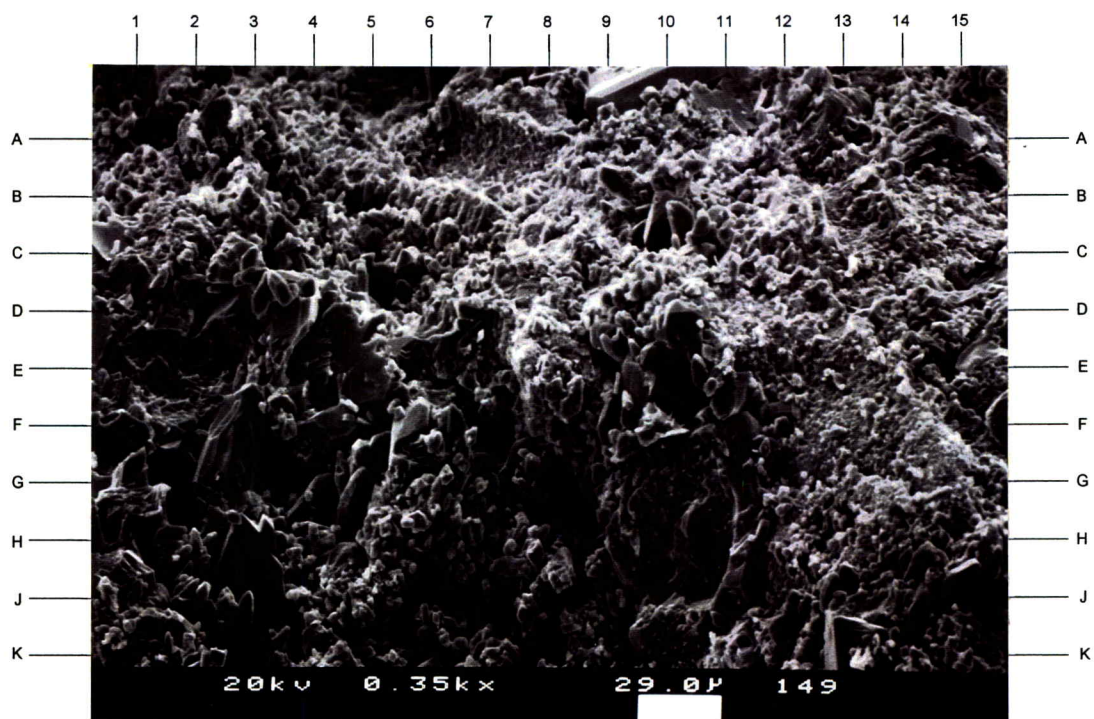
Depth: 2537.4 Feet

A

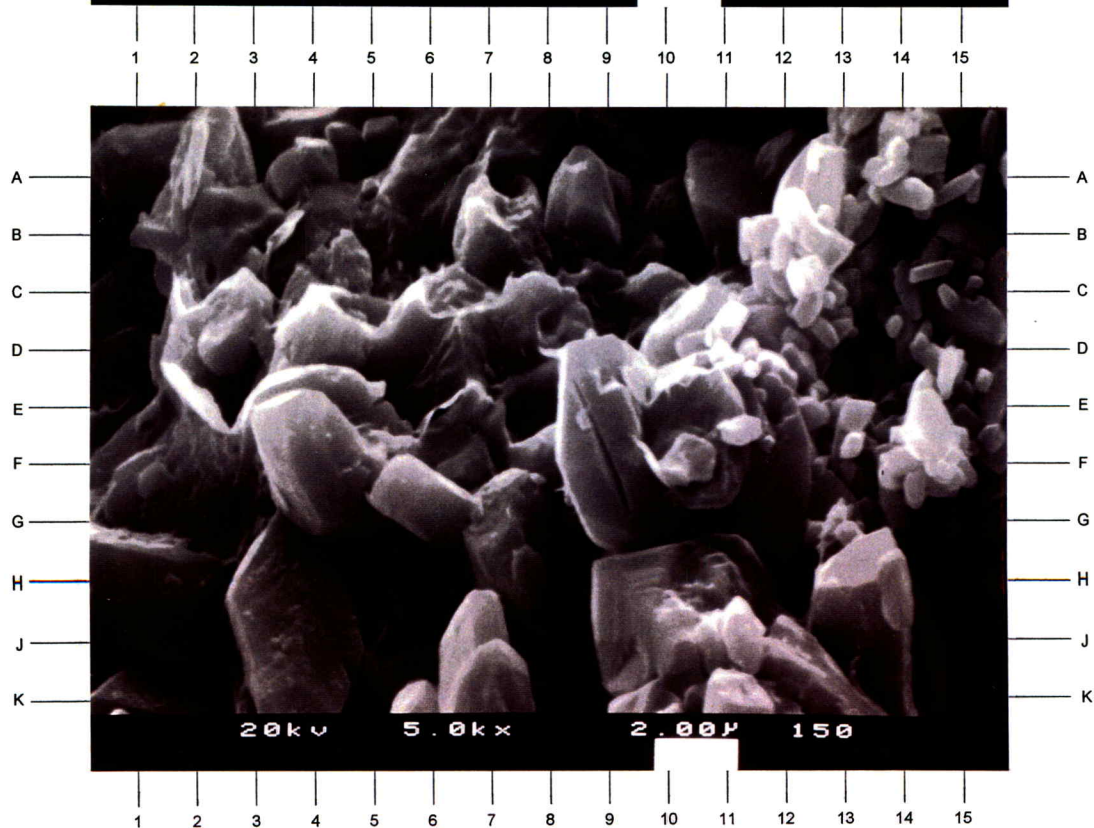
Authigenic quartz overgrowths appear on many very fine sand and silt grains (9-11 at top, D10, D-F4-5, H-K3), indicating much intergranular and interparticle pore space (G3.5, G-H8.5, E14.5) was available for the overgrowths to form. Much of the sample is calcite microspar to micrite, although some, more coarsely crystalline calcite is also present (D3, F-G2-3, B-C10). Minor quantities of dolomite were also observed in this sample. Skeletal allochems have been strongly micritized or recrystallized and are difficult to discern (A-C5-8, E-G12-15). (350X)

B

This is an enlargement of the area surrounding J4.5 in Plate 7A. The calcite crystals in this area of the sample are four to six microns in size, although some are less than one micron (A-F12-15). Most of the abundant micro-intercrystal pores (G-K5-6, G-K15) are free of pore lining materials, but traces of flaky or fibrous illitic clay are present (C2, B3.5, E6, D8). (5000X)



A



B

PLATE 8

SEM Photomicrographs

Sample 2A

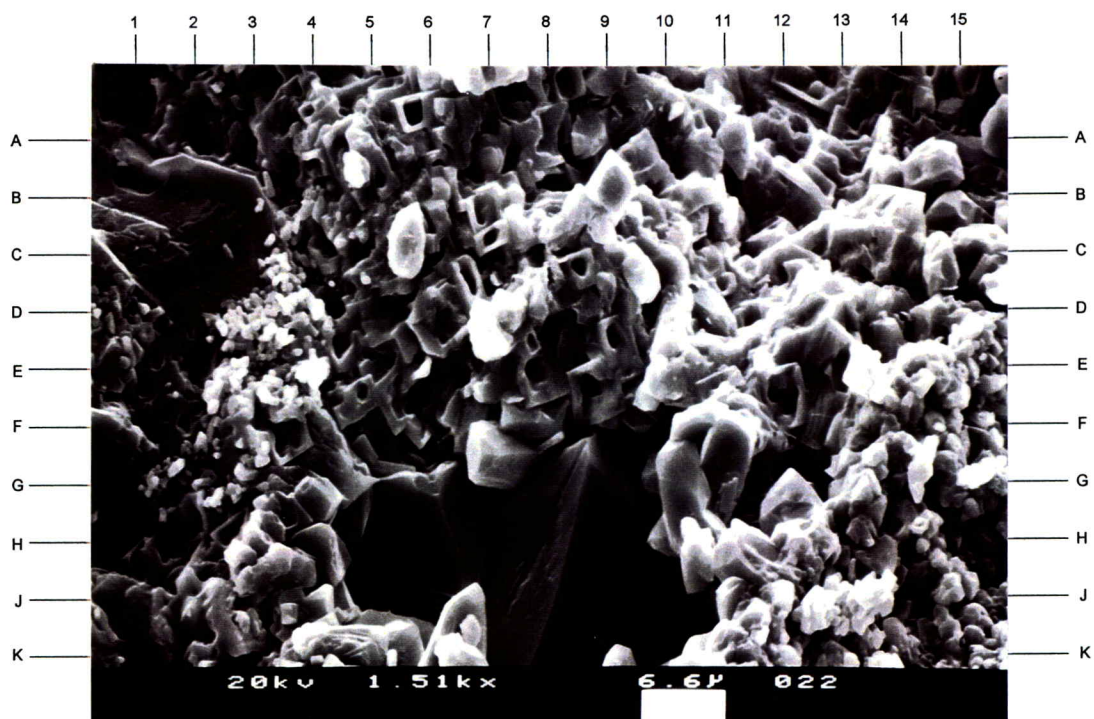
Depth: 2537.4 Feet

A

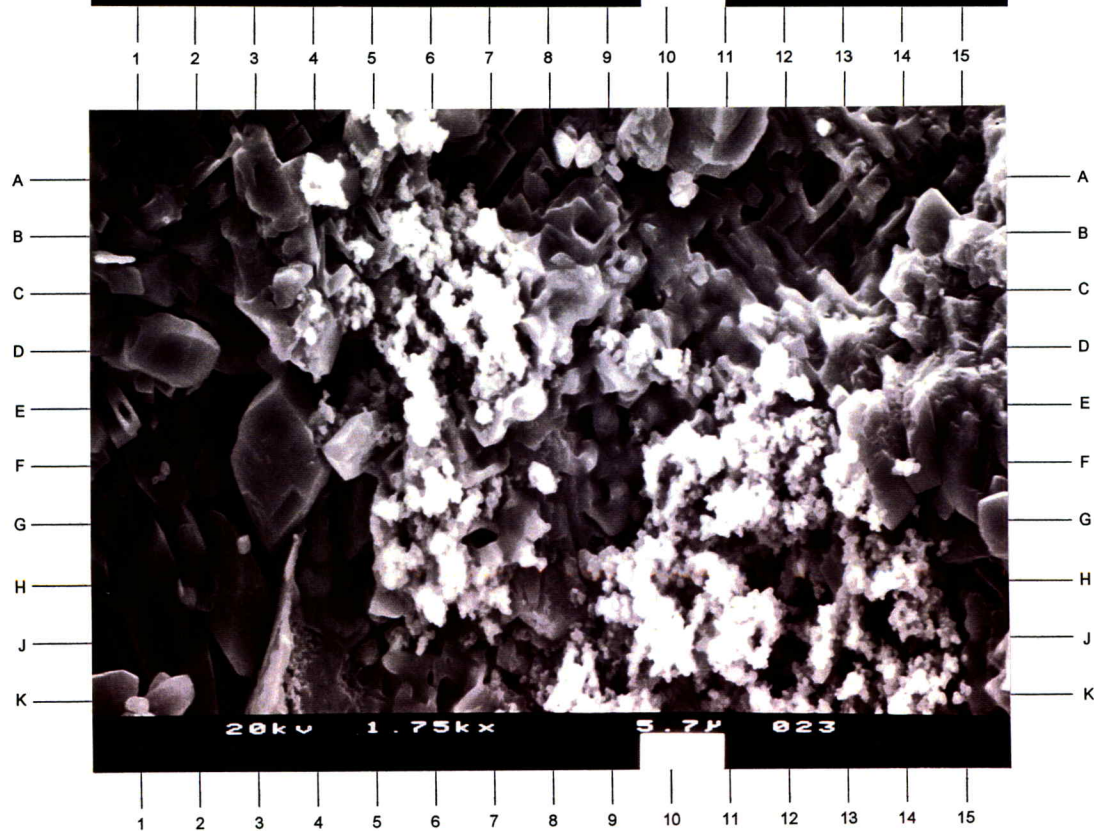
Minor patches of halite (top-F4-10) were discovered in the SEM analysis. X-ray diffraction analysis measured 0.5% halite in this sample. The individual cubic halite crystals are commonly hollow or partially dissolved. They seem to be natural authigenic crystals, rather than precipitates from formation waters or drilling fluids that formed during coring. Tiny calcite crystals have grown over some halite crystals at C-F3-4. Calcite microspar occupies the right-third of the photo, whereas finely crystalline calcite is present in the bottom-central portion. Quartz overgrowths are visible at B-D1-3 and E-H1-2. (1510X)

B

Another area of this sample, nearby that shown in Plate 8A, contains additional natural halite (A-C7-14). In this instance, microcrystalline silica has formed on top of halite at B-J5-7, indicating the halite was apparently present prior to the precipitation of the silica. Silica also fills a pore and coats calcite crystals within E-K9-15. (1750X)



A



B

PLATE 9

Thin Section Photomicrographs

Sample 3B

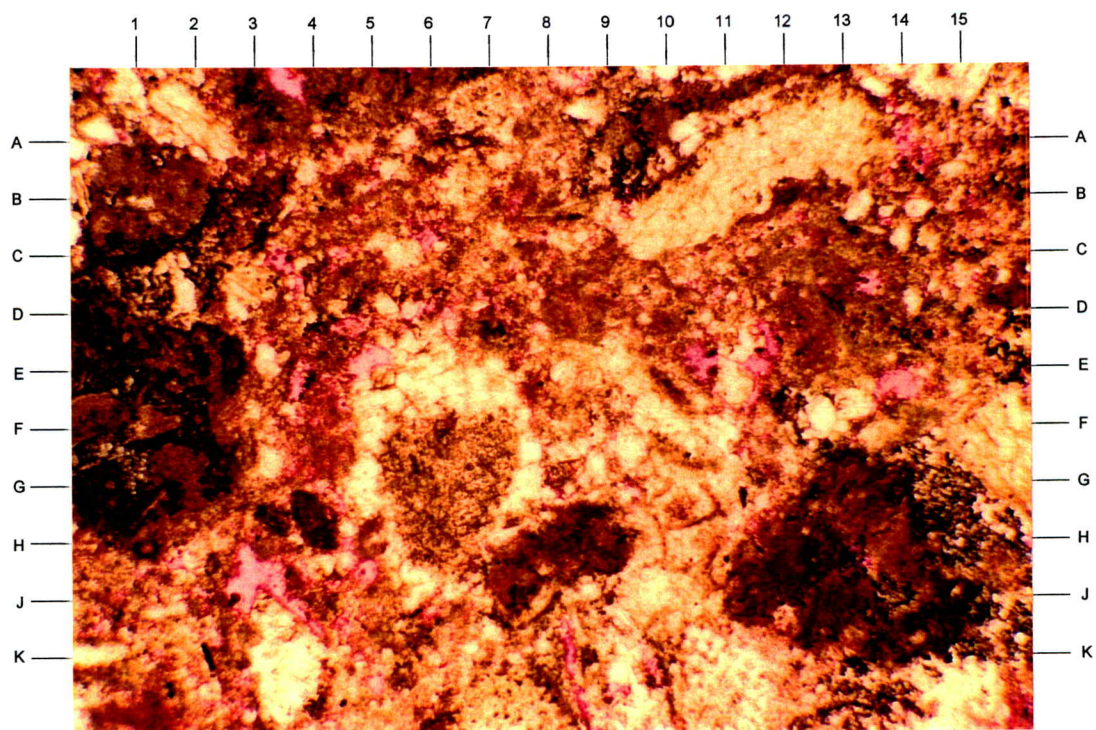
Depth: 2541.7 Feet

A

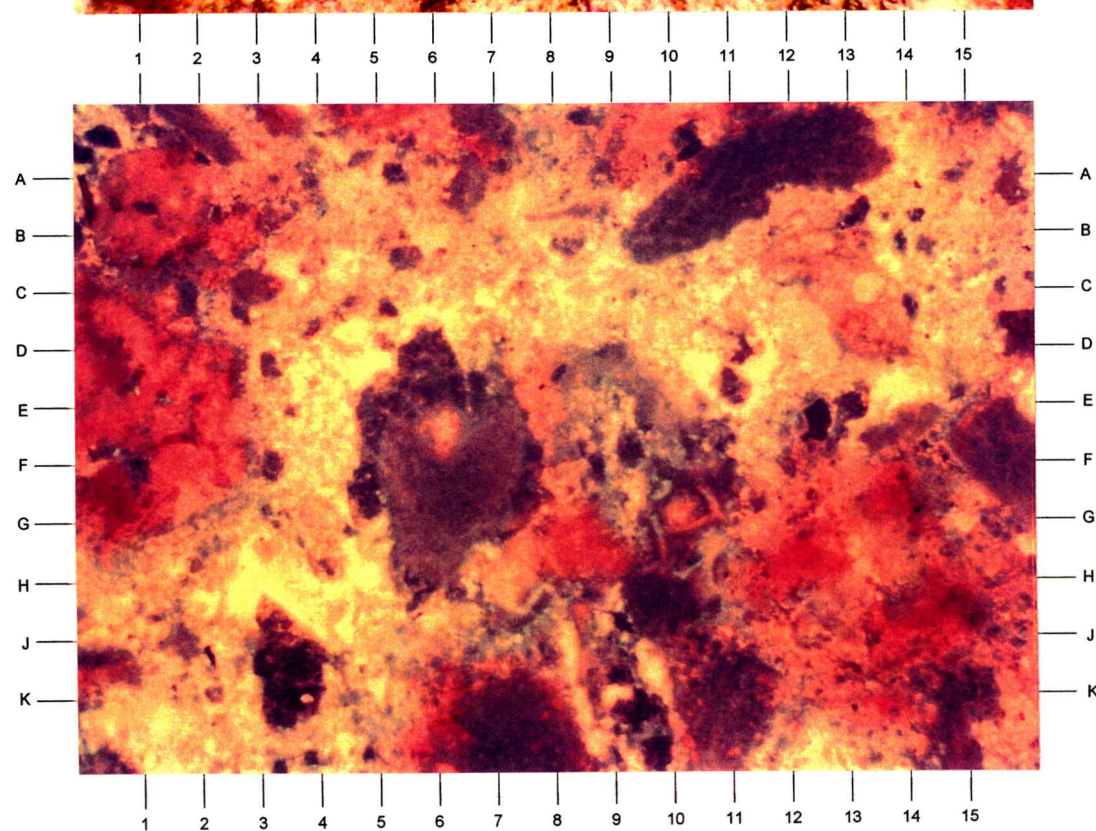
Rock Type:	Silty/sandy limestone
Rock Name: (Dunham, 1962) (Folk, 1980)	Silty/sandy peloid oncolite skeletal grainstone/packstone Silty/sandy peloid oncolite biomicrosparite
Average Allochem Size: (estimated)	0.32-0.50 mm (medium sand-size); range = 0.06-2.05 mm
Allochem Sorting:	Poor
Allochem Types:	Common algal oncolites (B1-3, D-H1-2, G-K12-15), peloids (H8, D8.5), echinoderms (G6, bottom-K7, K11), mollusks (A12?), foraminifers, bryozoans, and brachiopods; traces of possible intraclasts
Terrigenous Grains:	Fairly common silt to very fine sand (mainly quartz; minor potassium feldspar and plagioclase; traces of mica, rock fragments, and heavy minerals); traces of organic material
Matrix:	Original carbonate matrix, if any, has been neomorphosed to microspar
Authigenic Minerals:	Abundant calcite microspar (C-D10-11); minor finely to medium crystalline calcite (J-K3-4, E6); minor to trace amounts of dolomite, hematite, pyrite, quartz (including overgrowths), gypsum (XRD), anhydrite, clay minerals (SEM), chert, and halite (SEM); rare feldspar overgrowths and titanium oxide
Porosity Types:	Abundant intercrystal/interparticle and micro-intercrystal pores; minor to common intraparticle and moldic pores (H-J3); rare intergranular pores (pore space is impregnated with magenta-dyed epoxy)
Structures:	None apparent
Comments:	Very fine hematite is often concentrated around or within oncolites and micritized allochems; many skeletal grains are micritized (C-E12-14)
Magnification:	79X, transmitted light

B

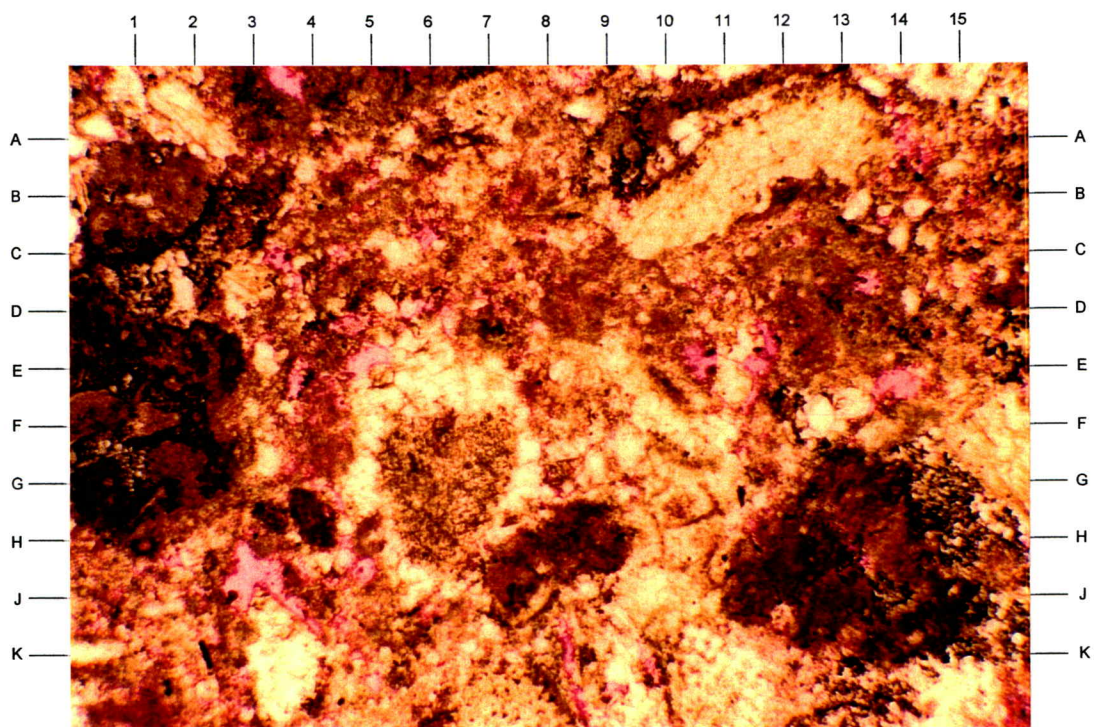
The areas of bright gold color indicate abundant pores, although the majority of pores are small intercrystal and micro-intercrystal pores. A more permeable pathway that connects larger pores and pores within microspar and micrite is visible along K1 to G4 to C4 to E14 to A15. Oncolites (reddish; A-G1-2, F-K12-15) contain some ineffective porosity, whereas crystalline allochems, cement, and sand/silt grains (all dark) contain virtually no porosity. Much irreducible water is probably associated with this sample. (79X, fluorescent light)



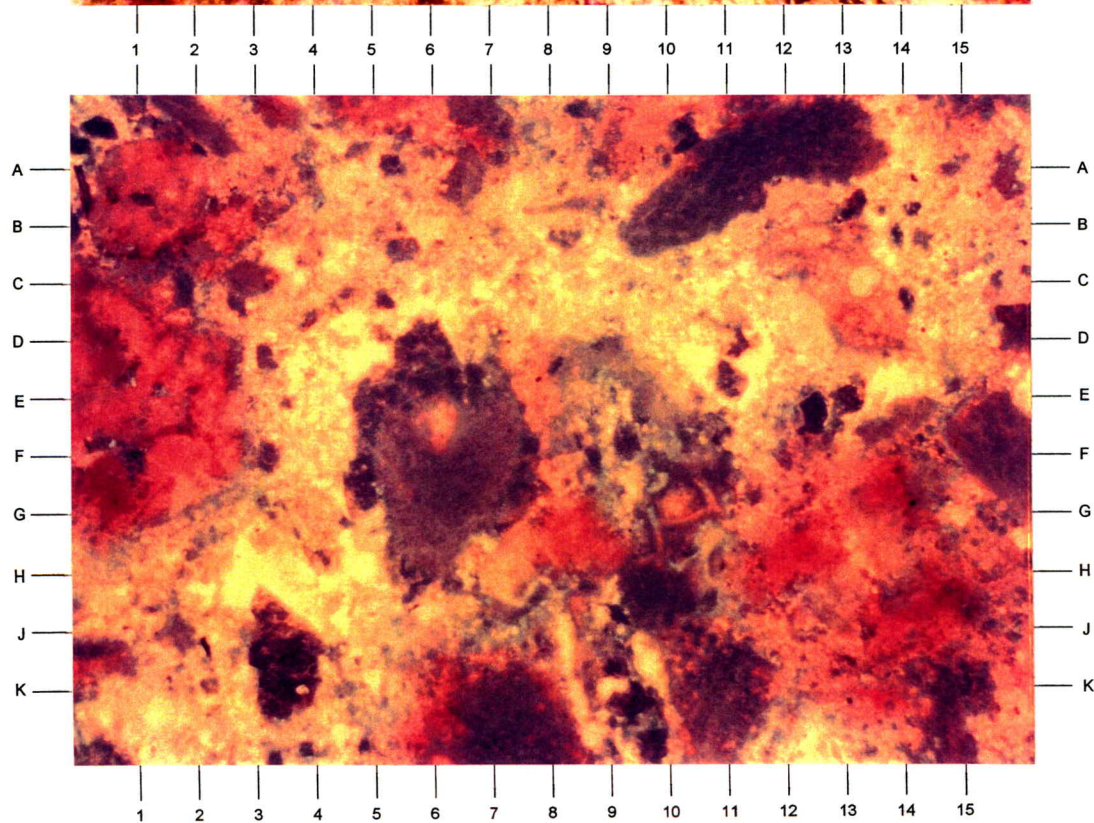
A



B



A



B

PLATE 10

Thin Section Photomicrographs

Sample 3B

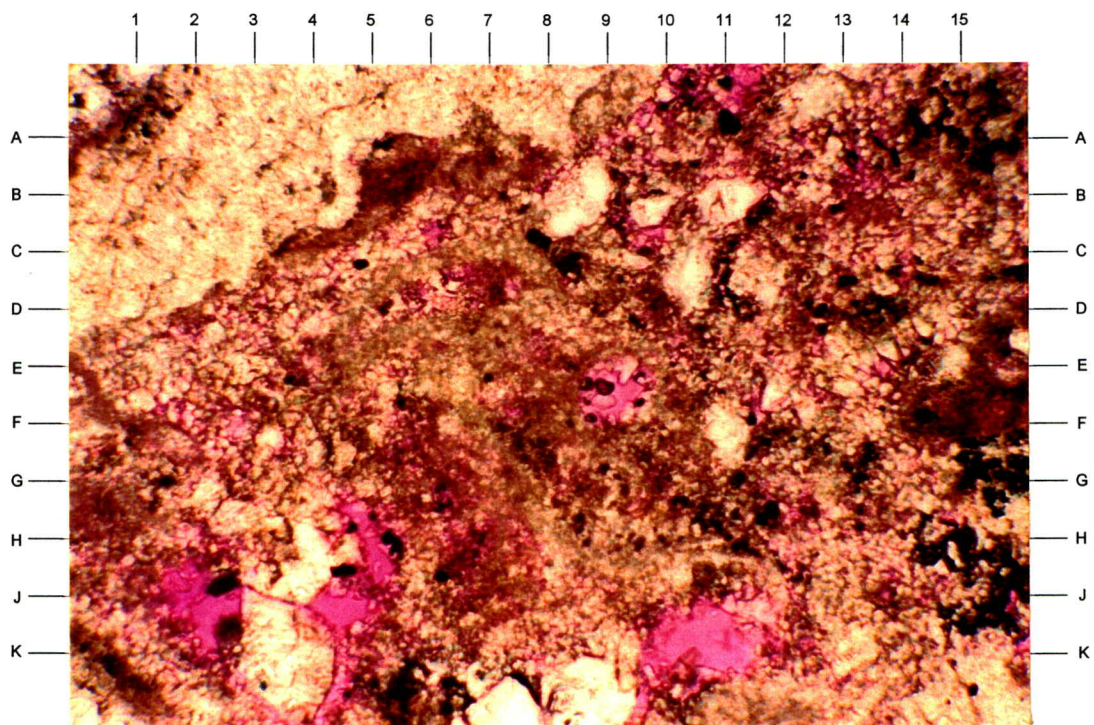
Depth: 2541.7 Feet

A

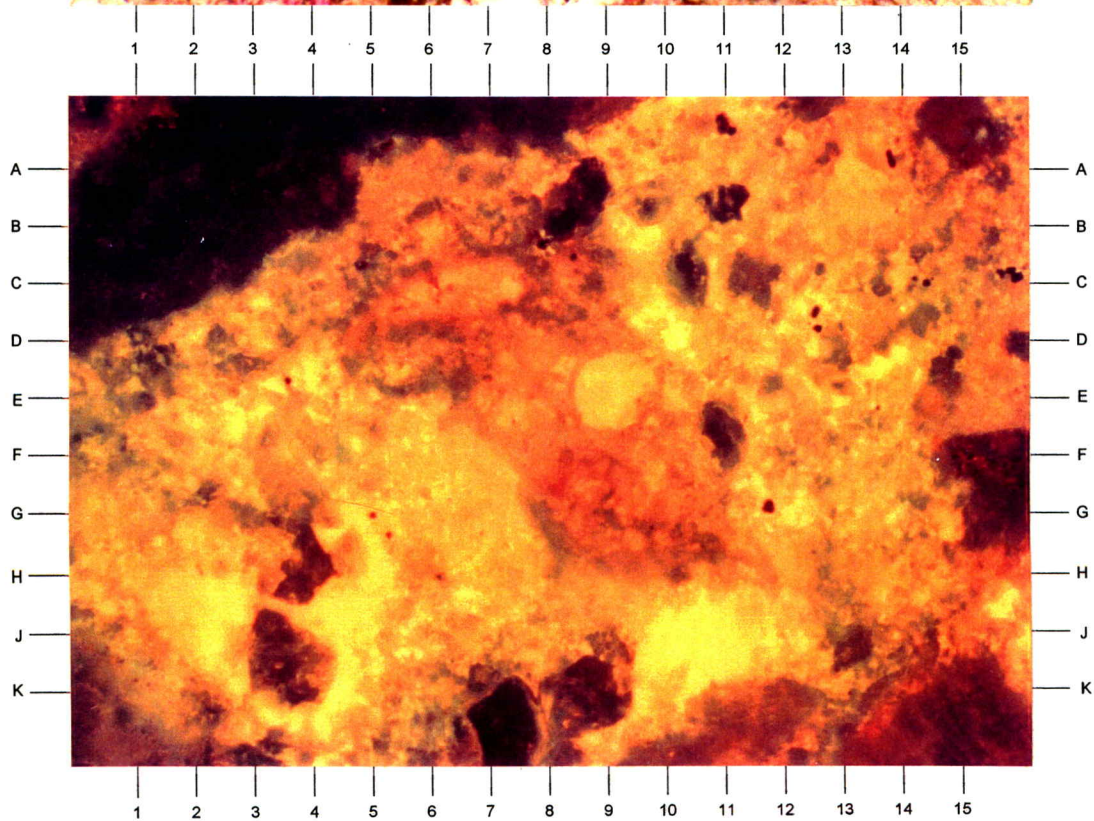
This photomicrograph shows the portion of Plate 9A surrounding C-D13. Along with the relatively larger pores (J-K2, E-F9, J-K10.5), abundant intercrystal and micro-intercrystal pores are apparent (D-G2-4, A-E12-14). Anywhere a magenta color is visible, pores have been impregnated. Notice that the interconnections among the larger pores are generally constrained to the very small pores. Most of the black specks in the view are authigenic pyrite crystals. (200X, transmitted light)

B

Porosity is highlighted by the bright gold glow of the fluorescent epoxy-impregnated pore system. Elements of the sample that remain dark include skeletal fragments (top-left corner), silt grains (A-B8.5, A-B11, C10.5, E-F11, bottom-K7.5), and coarser calcite cement crystals (J-K3.5, K8.5, F-G15.5). The remaining microspar and micritized allochems contain variable amounts of pore space, much of which may not be effective pore space. Permeabilities through the micro-intercrystal pore system will be low and bound water may be high. (200X, fluorescent light)



A



B

PLATE 11

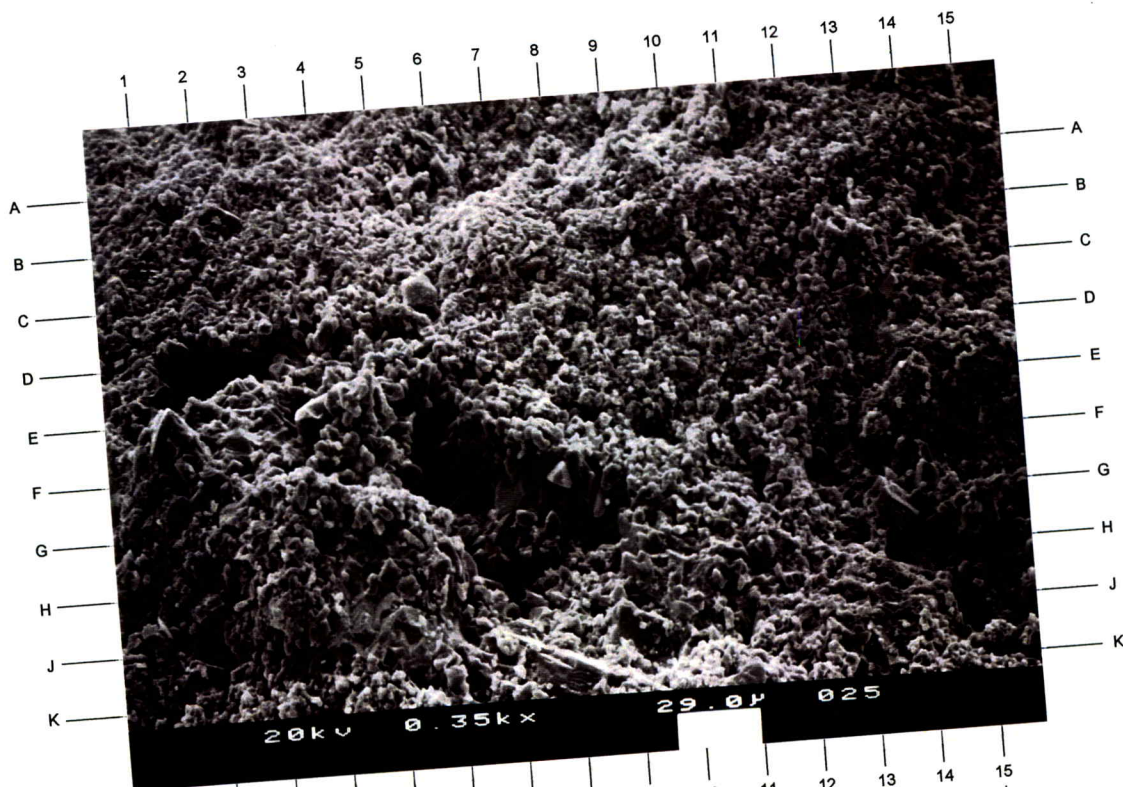
SEM Photomicrographs
Sample 3B
Depth: 2541.7 Feet

A

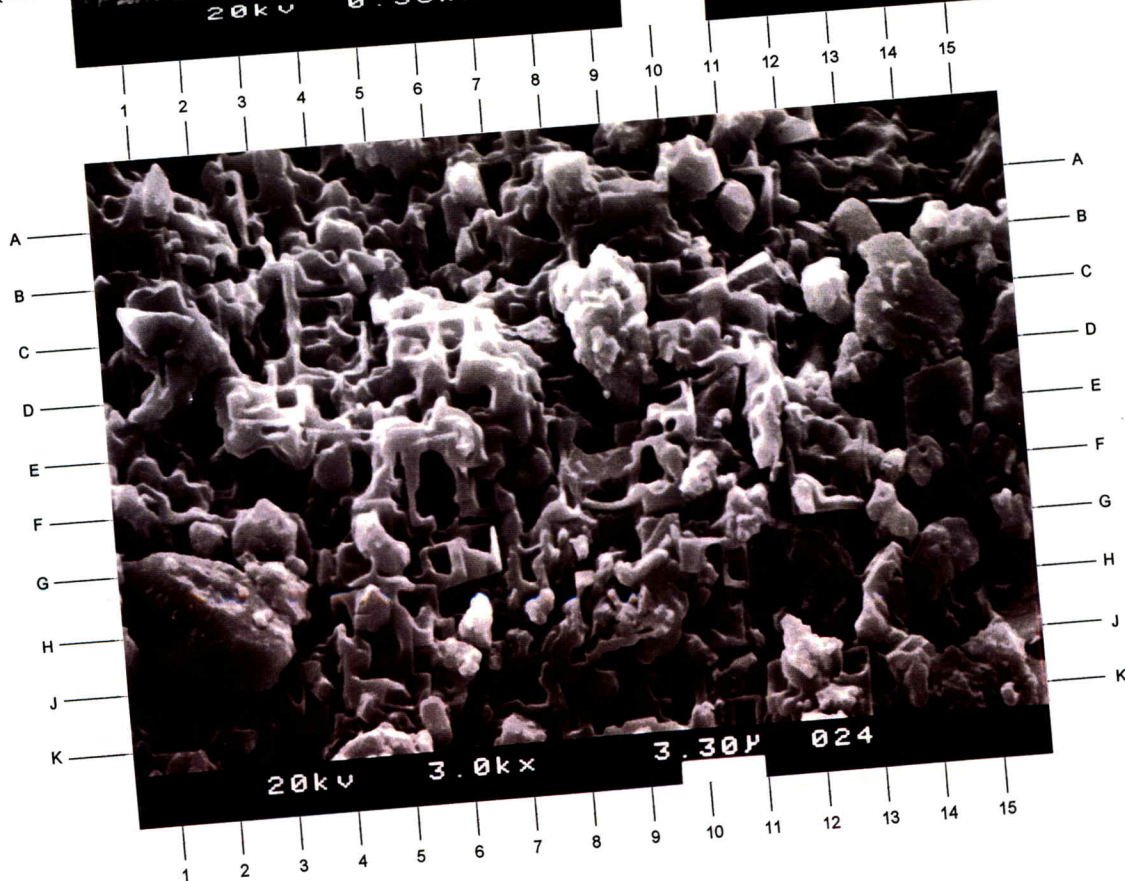
A large section of this area of the sample contains microcrystalline halite (much of the top half of this view). The bottom half of the view represents calcite with traces of dolomite (G-H13.5). Larger intercrystal pores appear at D-E2, F6, G-H8, and H-K15. These pores are interconnected by smaller intercrystal pores and micro-intercrystal pores within the microspar cement and micritized allochems. The halite also contains numerous micropores. (350X)

B

Under close examination, the halite (most of view) consists of tiny, incomplete crystals (e.g., A-E4, C-H6) that were never completely developed or have been partially dissolved. The morphology of the halite and its intimate association with calcite (H2, C9, A-B11) and dolomite (E14) may indicate that the halite is natural and not a precipitate that formed during coring. In any case, the fact that halite was not detected in thin section or by X-ray diffraction analysis shows that this mineral is a minor, sparsely distributed component of this sample. (3000X)



A



B

PLATE 12

SEM Photomicrographs

Sample 3B

Depth: 2541.7 Feet

A

In some areas of this sample, traces of authigenic illitic clay (C-D3.5, 11-12 at top, B13.5) are observed among the calcite microspar. The particles around G-H6.5, D11-12, and G12-13 have the composition of potassium feldspar. It is unclear whether they are direct precipitates or the remnants of dissolved, detrital potassium feldspar grains (see also Plate 13A). Authigenic pyrite and quartz appear at D12.5 and F-H10-11, respectively. (1900X)

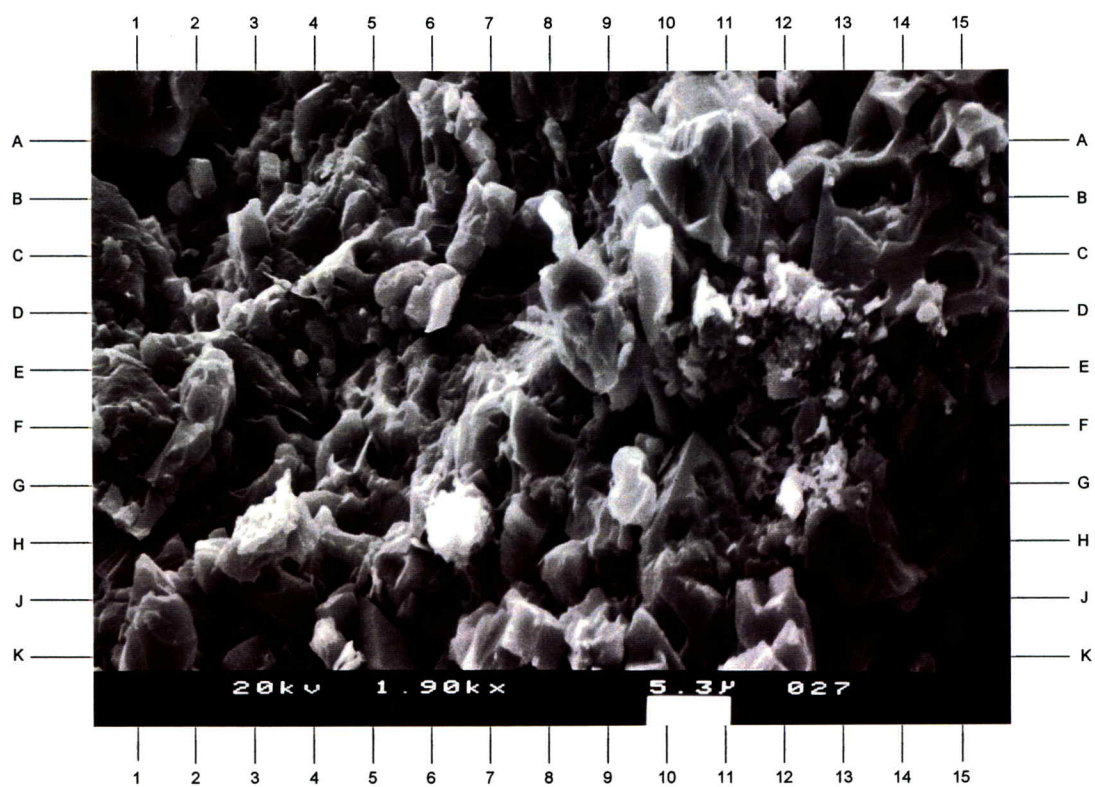


PLATE 13

SEM Photomicrographs

Sample 3B1

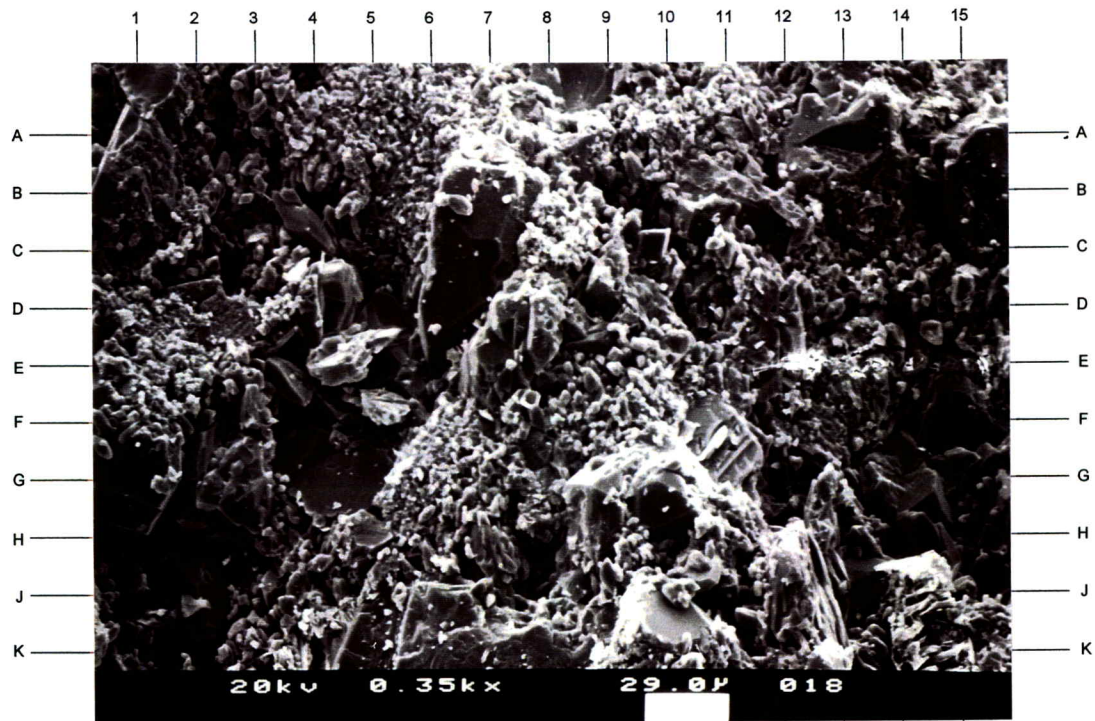
Depth: 2541.7 Feet

A

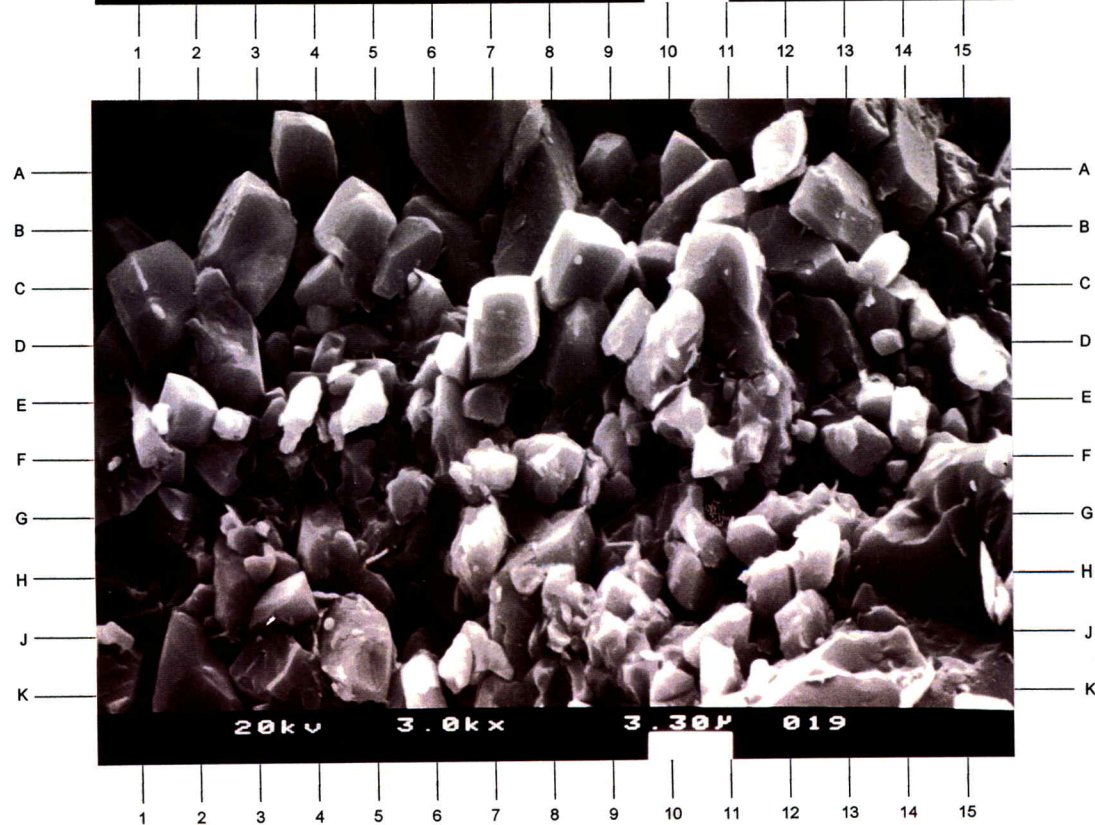
Because of the appreciable halite found in the previous SEM analysis of Sample 3B (Plate 11), this sample was analyzed again from an adjacent plug end, drilled in oil, taken from the center of the core. No halite was found in the subsequent analysis, showing that natural halite, if present, is not common and is sparsely distributed. A siltier portion of Sample 3B1 is shown here, revealing quartz grains with overgrowths (A-B1, B-E7, A13, G-H9-10), albite (F-G10-11), and probable, highly dissolved potassium feldspar grains (K4, J-K14-15). A rhombic, ferroan dolomite crystal appears at C9.5-10. Pore space is common but not well interconnected. (350X)

B

This is an enlargement of the area surrounding F9 in Plate 13A. Calcite crystals that are less than ten microns in size make up a large proportion of this sample. The crystal surfaces are smooth, and the abundant micro-intercrystal pores are generally free of other mineral precipitates. Traces of flaky to fibrous illitic clay are sometimes encountered (E10, G12.5-13, D-E5, C6). Although the micro-intercrystal pores are abundant, associated permeability will be low and irreducible water is likely to be high. (3000X)



A



B

ENERGY DISPERSIVE SPECTROSCOPY (EDS) PLOTS

TN-5400 Core Labs Dallas
Cursor: 0.190keV = 0

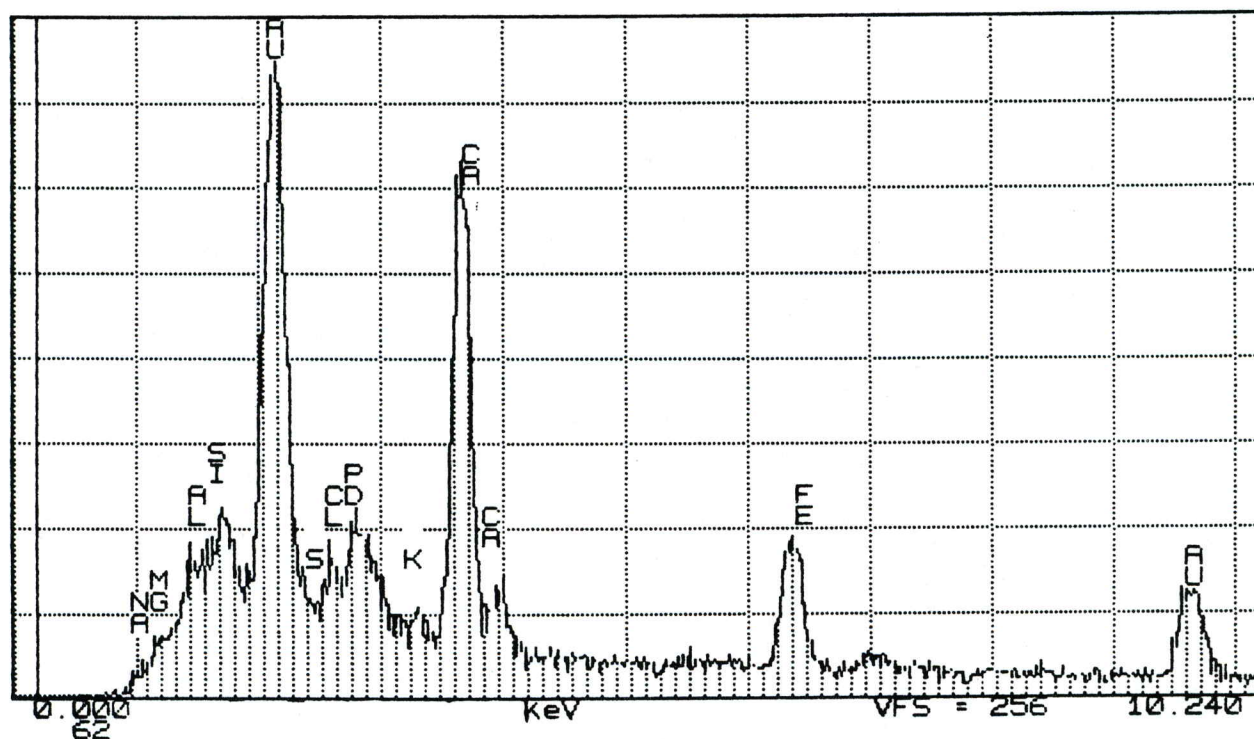


Figure 1. This is a spectral plot of the elemental composition of mixed-layer illite/smectite clay seen in Plate 4. Component elements are silicon, aluminum, iron, potassium, and magnesium. The large calcium peak is due to the predominant, underlying and surrounding calcite crystals. The gold and palladium peaks are due to the conductive coating added to the samples for SEM analysis.

TN-5400 Core Labs Dallas
Cursor: 0.180keV = 0

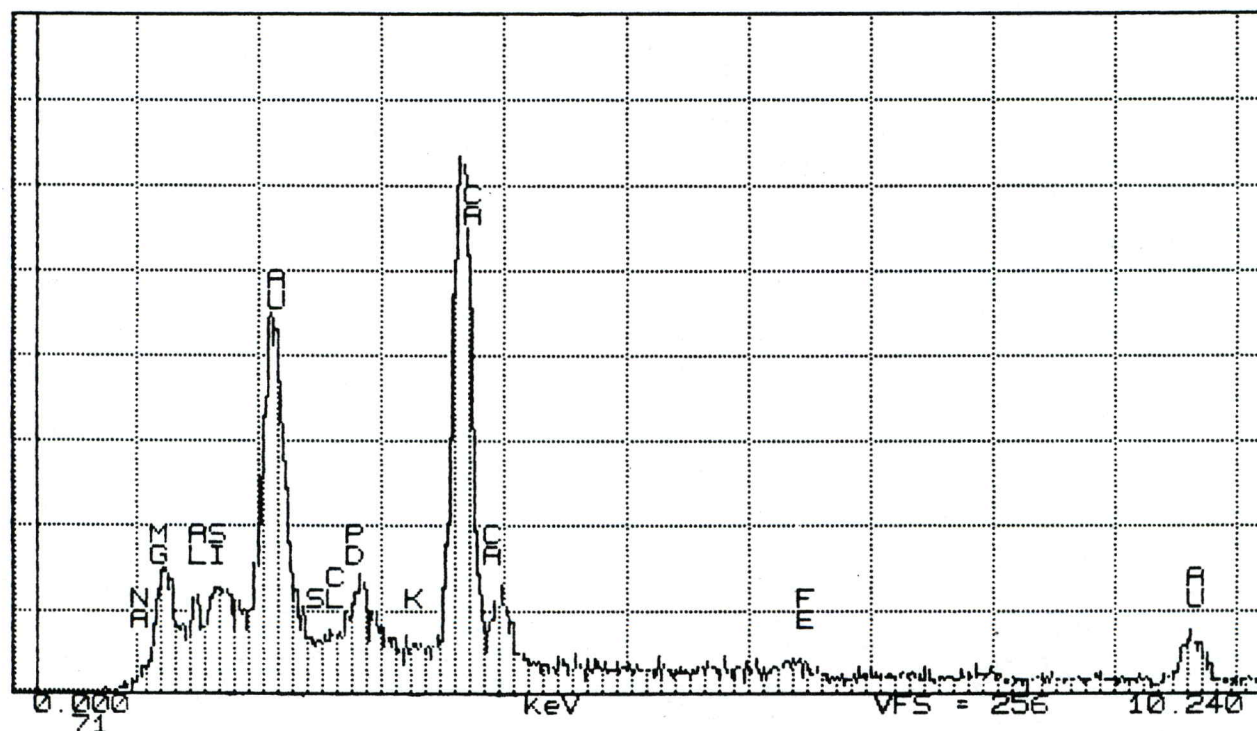


Figure 2. This EDS spectrum shows the composition of the dolomite crystal observed at A3 in Plate 4. Calcium and magnesium are the principle components. EDS analysis cannot detect elements lighter than sodium. The dolomite may contain trace amounts of iron. Higher iron content was found in other dolomite crystals. The lower silicon and aluminum peaks are due to interference from clays.

TN-5400 Core Labs Dallas
Cursor: 0.190keV = 0

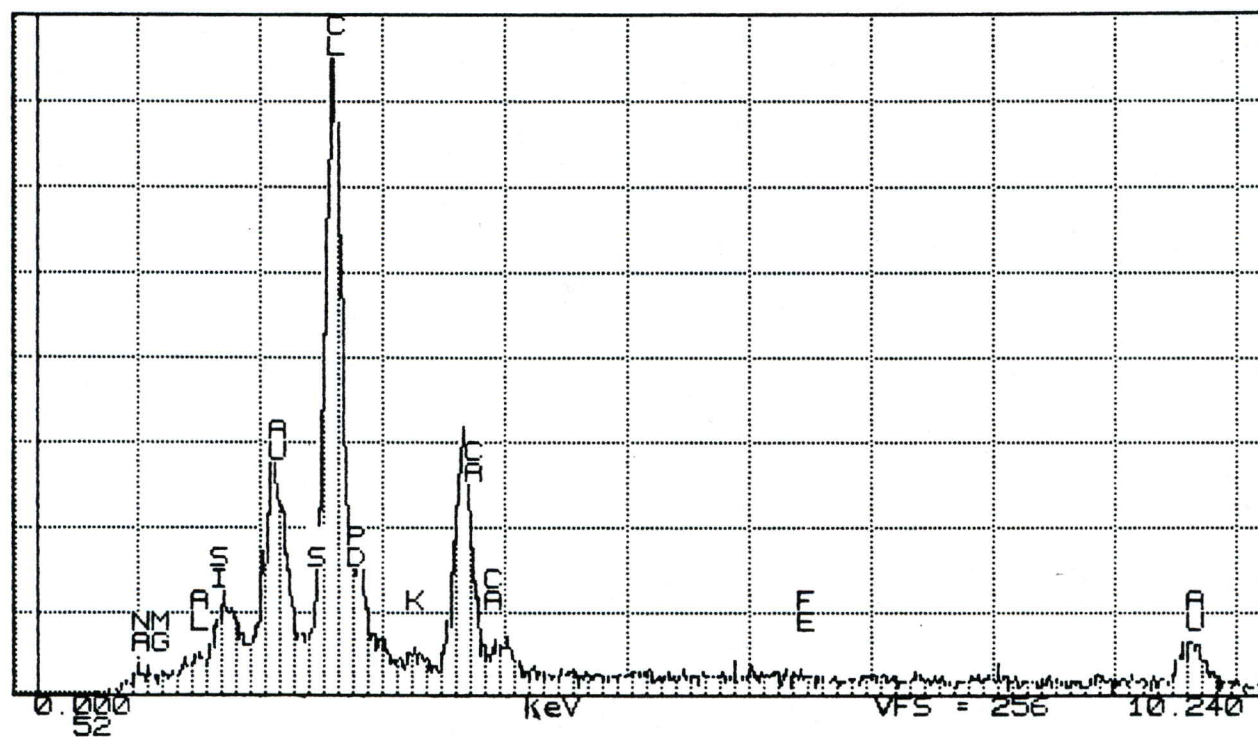


Figure 3. The high chlorine peak and low sodium peak are indicative of halite. Sodium is difficult to detect with EDS analysis. This is an elemental spectrum of the halite seen on Plate 8A. Interference from calcite and quartz, which are also present in Plate 8A, has produced peaks of calcium and silicon.

TN-5400 Core Labs Dallas
Cursor: 0.190keV = 0

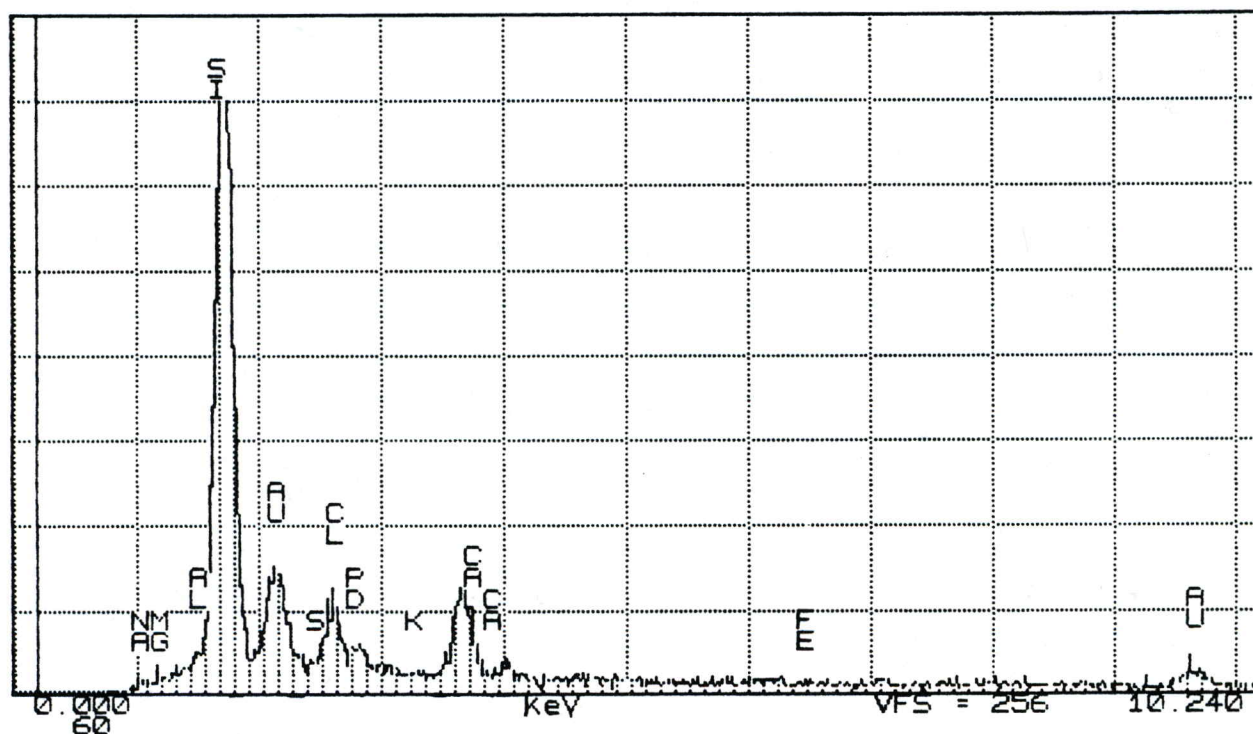


Figure 4. Plate 8B shows some very fine material coating halite crystals and partially filling a pore. This material is confirmed to be silica by this EDS plot. Notice the dominant silicon peak, with interference from calcite and halite producing smaller calcium and chlorine peaks, respectively.

TN-5400 Core Labs Dallas
Cursor: 0.190keV = 0

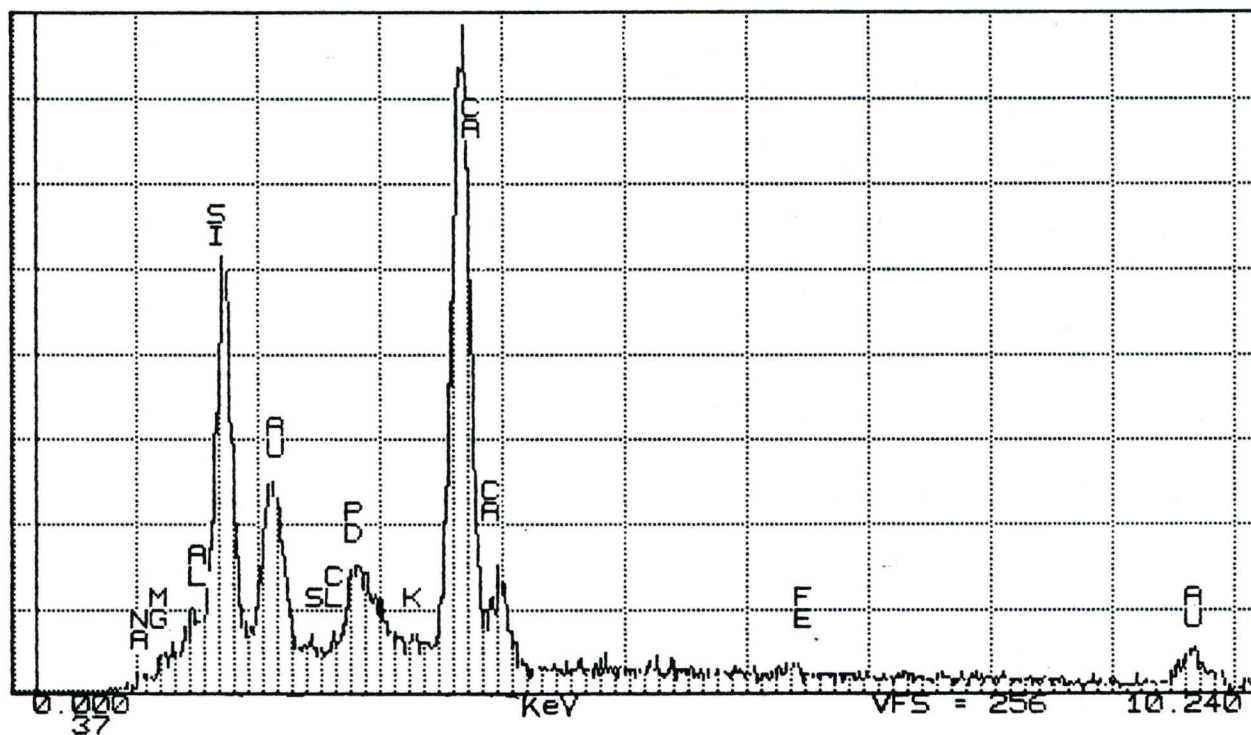


Figure 5. This EDS plot shows the overall elemental composition of Sample 3B1 (Plate 13) as was observed at 100X magnification. Elements lighter than sodium are not detected. The principal elements are calcium (from calcite and lesser dolomite) and silicon (mainly from detrital, siliciclastic grains). Lesser amounts of aluminum, magnesium, and potassium are represented. Trace amounts of chlorine, sulfur, iron, and sodium may also be present.

TN-5400 Core Labs Dallas
Cursor: 0.190keV = 0

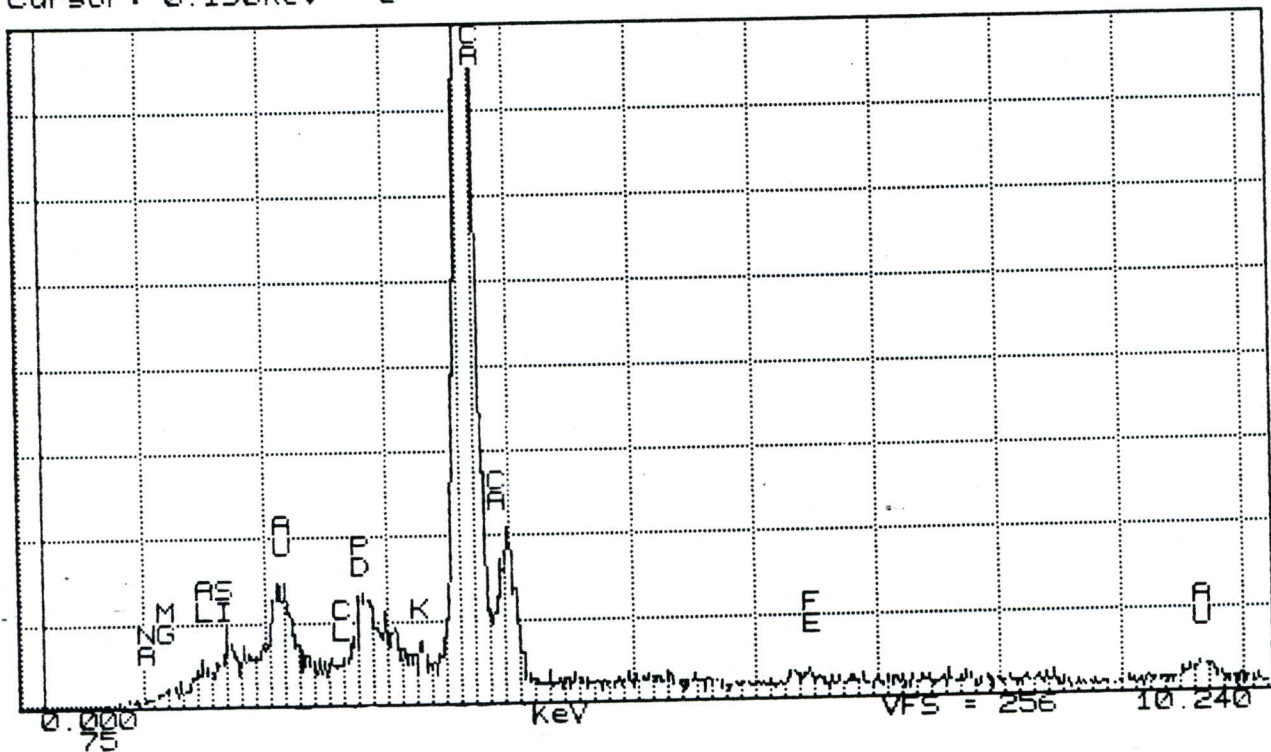


Figure 6. This plot attempts to show the composition of the flaky, authigenic clay seen at E10 in Plate 13B. It is impossible to isolate these small crystals; thus, the largest peak (calcium) is produced by the predominant calcite. The remaining peaks, discounting the gold and palladium coating, are silicon, aluminum, and potassium, with possible traces of iron and magnesium. These elements, combined with the flaky to fibrous morphology, represent an illitic clay.